Blatt, Stephen Robert

TEST OF TIME REVERSAL INVARIANCE IN POSITIVE KAON(MU3) DECAYS

Yale University

PH.D. 1981

PLEASE NOTE:

In all cases this material has been filmed in the best possible way from the available copy. Problems encountered with this document have been identified here with a check mark __✓__.

1. Glossy photographs or pages _____
2. Colored illustrations, paper or print _____
3. Photographs with dark background _____
4. Illustrations are poor copy _____
5. Pages with black marks, not original copy _____
6. Print shows through as there is text on both sides of page _____
7. Indistinct, broken or small print on several pages __✓__
8. Print exceeds margin requirements _____
9. Tightly bound copy with print lost in spine _____
10. Computer printout pages with indistinct print _____
11. Page(s) _____ lacking when material received, and not available from school or author.
12. Page(s) _____ seem to be missing in numbering only as text follows.
13. Two pages numbered _____. Text follows.
14. Curling and wrinkled pages _____
15. Other _____

Test of Time Reversal Invariance In $K^{+}_{\mu 3}$ Decays

A Dissertation

Presented to the Faculty of the Graduate School

of

Yale University

in Candidacy for the Degree of

Doctor of Philosophy

by

Stephen Robert Blatt

December 1981

ABSTRACT

Test of Time Reversal

Invariance In $K^+_{\mu 3}$ Decays

Stephen Robert Blatt

Yale University

1981

We have measured the transverse polarization of muons from the decay $K^+ \rightarrow \pi^0 \mu^+ \nu_\mu$, in an experiment conducted at the Brookhaven National Laboratory AGS. A violation of CP (or T) invariance in the $K_{\mu 3}$ decay produces a component of polarization normal to the decay plane. One class of theories of CP violation predicts this polarization out of the decay plane to be small but measurable, while other theories predict a null result.

A 4 GeV non-separated positively charged beam was produced at zero degrees with respect to a 29.2 GeV external proton beam colliding on a platinum target. A cylindrically symmetric detector, consisting of scintillation counter hodoscopes, a focusing magnet-energy degrader, and a polarimeter, was used to detect and track the muon from the $K^+_{\mu 3}$ decay. The muons were stopped in the polarimeter, where a 55 gauss field was applied to cause the muon spin to precess. The subsequent muon decay to $e^+ \nu_\mu \nu_e$ allowed the polarization of the muons to be determined by measuring the asymmetry of the direction of the emitted positron. The neutral pion, created in the $K^+_{\mu 3}$ decay, decayed into two gammas, one of which was detected in the lead glass array, defining the event.

We collected 20.8 million events and obtained for the CP violating component of polarization, normal to the decay plane, $P_n = -0.0031 \pm 0.0053$. The parameter $\mathrm{Im}\xi$, with ξ the ratio of the form factors in the $K_{\mu 3}$ decay, is found to be -0.016 ± 0.027, not significantly different from the CP conserving value of zero. The average value of the ratio of the normal to transverse components of the muon polarization in the kaon rest frame is $\phi = \langle P_n / P_t \rangle_{CMS} = -0.0063 \pm 0.0108$. Our null result places important constraints on models of CP violation involving the exchange of Higgs bosons.

TABLE OF CONTENTS

Acknowledgements

Many people have contributed to the research reported in this paper; I can only mention here a few. The work reported herein was Experiment 735 at the Brookhaven AGS. The assistance of the staff of the AGS and their ability to do almost anything in short order to further the experiment was greatly appreciated. I would also like to acknowledge the hospitality of the Brookhaven Physics Department, where most of this report was written.

Andy Gangemella and Warren Jappe were indispensable in the construction and maintenance of the experimental apparatus. The precision nature of the experiment required accurate and precise work on their part, and they ably rose to the challenge. Tom Rudolf and Don Makowiecki contributed much to the development of the FASTBUS electronics system.

Kevin Black contributed greatly during the debugging and data taking phases of the experiment. William Morse and Larry Leipuner assisted me in the construction of the time-to-digital converter as well as in many other areas of the experiment. They also served as gracious guides to Long Island's South Shore.

Richard Larsen supervised the construction of the detector apparatus and the mechanical requirements of the electronics with a firm and steady hand on the tiller. Michael Schmidt contributed greatly and was always available for advice and encouragement. His assistance in reviewing drafts of this report was timely and helpful.

Myron Campbell's contributions were innumerable. His as-

sistance in the design and building of the electronics, in the computer programming for the data analysis, and in helping to implement, on the UNIX system, the typesetting requirements for this report, was particularly appreciated.

My advisers, Robert Adair and Henry Kasha, provided great insight into the field of high energy physics. It was a privilege to work with them and learn from them.

I. Theory

A. Violation of CP Invariance

Violation of CP invariance was discovered in 1964 when the decay $K_L \to 2\pi$ was first observed[1]. The nature of this violation is still not well understood. We report here on a search for violation of CP invariance in $K^+_{\mu 3}$ decays. Our experiment is an order of magnitude more precise than the previous measurements on the $K^+_{\mu 3}$ decay, and is of somewhat higher precision than achieved in a recent search for CP violation in $K^o_{\mu 3}$ decays. To this date the only observed CP violation is in the $K_L \to 2\pi$ decay, with a branching ratio[2] of $2.589 \pm 0.060 \times 10^{-3}$ and in the charge asymmetry ratio of K^o_{13} decay[2],

$$\delta = \frac{(K_{1^+3} - K_{1^-3})}{(K_{1^+3} + K_{1^-3})} = 3.30 \pm 0.12 \times 10^{-3},$$

both of which can be expressed by the same complex parameter, ε, with[3] $|\varepsilon| = 2.27 \pm 0.08 \times 10^{-3}$.

Several theories of CP violation[4] have been developed based on quantum chromodynamics(QCD) and the gauge theory of electro-weak interactions. When the parameters of these theories are adjusted to fit the observed data, they yield varying predictions for other phenomena in which CP violation might be observed, such as a non-zero value for a second parameter ε', related to the charged-neutral ratio in the two pion decay from K_S and K_L decays, a non-zero value for the electric dipole moment of the neutron, and an out-of-the-decay plane component of muon po-

larization in K_{13} decays. The physics of heavy quarks may also provide opportunities to observe violations of CP invariance, in the analogues of the K^o-$\overline{K^o}$ system for heavier quarks (the D, B and T systems) and in the branching ratios of particles with heavier quarks. We discuss below the various theoretical models and their predictions for some of these phenomena, deferring discussion of CP violation in $K_{\mu 3}$ decay until after we have discussed the $K_{\mu 3}$ decays in detail in the next section.

The standard six quark model (the Kobayashi-Maskawa model)[5] introduces a 3 x 3 generalized Cabibbo matrix which mixes the d, s, and b quarks. This 3 x 3 matrix is defined completely by three Cabibbo-like angles θ_1, θ_2, and θ_3 and a phase factor $\exp(i\delta)$ where the phase angle δ cannot be rotated away by redefining the quark fields. A non-zero value of δ generates CP violation. The 3 x 3 matrix reduces to a 2 x 2 matrix describing the u, d, s, and c quarks for $\theta_2=\theta_3=0$. The success of the Cabibbo theory with a single angle, the only angle which appears in the 2 x 2 Cabibbo matrix, in explaining low energy phenomena places severe limits on the size of the angles θ_2 and θ_3. In interactions involving the four lighter quarks (u,d,s,c), the CP violating angle δ appears only in the matrix element connecting the c and s quarks. When no c quark is involved, CP violation can take place in this model only when the heavier quarks participate via off-shell transitions. Thus, we expect CP violation to be uncommon at lower energies as we observe it to be.

From the size of ϵ, we find the combination of unknown angles $\sin\theta_2\sin\theta_3\sin\delta \simeq 10^{-3}$. The smallness of this factor implies

that CP violation in other low energy systems is at a very small level. The electric dipole moment of the neutron is estimated[6] to be of order 10^{-34}e-cm. The parameter ε', the parameter governing the 2 pion charged to neutral decay ratio in the neutral kaon system, has been estimated[7] in this model to be in the range 0.02ε to 0.002ε. The contribution to ε' comes from certain diagrams involving QCD corrections (called "penguin" diagrams) and the analysis of some of the factors involved is not clear. The current experimental value for ε'/ε is[3] 0.01 ± 0.04, and for the neutron electric dipole moment[8], $2.3\pm2.3\times10^{-25}$e-cm.

Another model of CP violation based on the standard model sets the CP violation from the Kobayashi-Maskawa matrix equal to zero and introduces all the CP violation in the Higgs sector, by introducing either two[9] or three[10] Higgs doublets. The two Higgs model is a soft CP violating model: that is, the Lagrangian conserves CP and the violation occurs via the spontaneous symmetry breaking in the Higgs sector. In soft models, the CP violation varies with energy. A hard model, such as the Kobayashi-Maskawa model outlined above, introduces CP violation in the Lagrangian. The absence in a natural way of flavor changing neutral currents, called natural flavor conservation, is a desirable feature to be included in gauge theories. To obtain soft models with natural flavor conservation, three Higgs doublets are needed[11].

The CP violating constant in a Higgs theory is $G_F m_q^2/m_H^2$, with m_q an effective quark mass and m_H the mass of the Higgs bosons. In the two Higgs model, with the mass of the Higgs boson equal to that of the W boson, there are severe problems with neu-

tral strangeness changing currents and with the predicted value of ε', both of which can be resolved only by imposing certain symmetries artificially on the Lagrangian or by adding a third Higgs doublet.

For a two Higgs model with $m_H \approx 1$ TeV, these problems disappear. The neutral strangeness changing rates are predicted to be several orders of magnitude below the observed rate, and $\varepsilon'/\varepsilon \approx 0.0005$. The electric dipole moment of the neutron is predicted to be approximately 10^{-26} e-cm.

The three Higgs model includes two Higgs doublets which couple to quarks and one which couples only to leptons. The vacuum expectation value of the product of these doublets can be complex, which leads to the CP violation. Since Higgs bosons couple to the mass of the fermions, CP violation will be more pronounced in systems with heavier quarks. The CP violating coupling is $G_F m_q^2/m_H^2$. To produce the observed CP violation in the K^o system, we must have a Higgs mass around 15 GeV if one calculates using effective quark masses, or, if one uses current algebra quark masses, a bare Higgs mass $m_o = 2$ GeV and an observed Higgs mass $m_H^2 = 15$ GeV. This leads to a neutron electric dipole moment of around[12] 10^{-25} e-cm. Recent calculations[13] of penguin diagrams in this model obtain values of ε'/ε of order 0.05, as compared with the experimental value[3] of 0.01 ± 0.04.

There are also gauge theories of the form[14] $SU(2)_L \times SU(2)_R \times U(1)$, with both left and right handed currents, and both a W_L and a W_R boson. To account for the observed parity violation at observed energies, the W_R boson mass is greater than

the W_L mass. Although violation of natural flavor conservation occurs in this model, the violation can be suppressed to the same order as right handed currents are suppressed. The CP and P violating terms in the Lagrangian imply $\varepsilon'=0$ and a small neutron electric dipole moment ($\approx 10^{-29}$ e-cm). CP violation may also take place via the Higgs mechanism or in the Kobayashi-Maskawa matrix. In the Higgs case, the observed constraint on ε' demands the Higgs coupling to be less than $G_F x 10^{-4}$, which leads to an electric dipole moment of approximately 10^{-24} e-cm.

These various theories are not mutually exclusive, as violation of CP invariance could occur via more than one mechanism. A large neutron electric dipole moment, for instance, would not necessarily rule out the Kobayashi-Maskawa model as the moment may be due to a Higgs contribution, while the Kobayashi-Maskawa mechanism might predominate in, perhaps, the heavy quark systems. Thus all of the possible interactions in which CP violation might take place should be explored.

B. K_{13} Decays

The K_{13} decays have been studied for many years. A rich variety of phenomena can be investigated, which give information on both the strong and weak interactions.

The matrix element for a semi-leptonic decay can be written in the form[15]:

$$M = \frac{G_F}{\sqrt{2}} \sin\theta_c \langle B|J^\lambda|A\rangle \langle v|j_\lambda|1\rangle$$

where $G_F = 10^{-5} M_p^{-2} (GeV)^{-2}$ is the Fermi coupling constant and

$\langle \nu | j_\lambda | l \rangle$ is the leptonic current. We can write the leptonic current exactly as $\bar{u}_\nu \gamma_\lambda (1+\gamma^5) v_\mu$ if we assume a pointlike lepton interaction, which is consistent with all experiments to date.

The exact form of the hadronic current $\langle B | J^\lambda | A \rangle$ is unknown, but we can write it in terms of form factors. These form factors can be functions only of the Lorentz invariants available, such as $q^2=(p_K-p_\pi)^2$, the momentum transfer in the decay. Experiments have shown that the hadronic current in the particular case of K_{13} decays displays only vector coupling, in the form expected from conventional V-A coupling.

The most general form for $\langle \pi | J^\lambda | K \rangle$ is $f_1(q^2)p_K+f_2(q^2)p_\pi$, where f_1 and f_2 are form factors. We can choose another set of form factors $f_\pm=\frac{1}{2}(f_1+f_2)$ and rewrite the hadronic term as

$$\langle \pi | J^\lambda | K \rangle = \{ f_+(q^2)(p_K+p_\pi)^\lambda + f_-(q^2)(p_K-p_\pi)^\lambda \}$$
$$= f_+(q^2)[(p_K+p_\pi)^\lambda + \xi(q^2)(p_K-p_\pi)^\lambda]$$

with $\xi=f_-/f_+$. CP violation will occur if the form factors f_- and f_+ have a relative phase between them, i.e. if ξ is complex. The magnitude of Im ξ is thus a measure of the CP violation in the K_{13} decay.

Due to e-μ universality, the $K_{\mu 3}$ and K_{e3} form factors are exactly the same, but because of the lighter mass of the electron, the form factor f_- is not involved in K_{e3} decays, to first order in m_e/m_K.

Consider the term of M proportional to f_-:

$$M_- = \frac{G_F}{\sqrt{2}} \sin\theta_c f_-(p_k-p_\pi)^\lambda \bar{u}_\nu \gamma_\lambda (1+\gamma^5) v_l$$

With $p_K - p_\pi = p_1 + p_\nu$ by conservation of momentum, we have

$$M_- = \frac{G_F}{\sqrt{2}} \sin\theta_c f_- \bar{u}_\nu (\not{p}_1 + \not{p}_\nu)(1+\gamma^5) v_1$$

From the Dirac equation we have $u_1 \not{p}_\nu = 0$, and $\not{p}_1(1+\gamma^5)v_1 = (1-\gamma^5)\not{p}_1 v_1 = (\gamma^5 - 1) m_1 v_1$, so

$$M_- = \frac{G_F}{\sqrt{2}} \sin\theta_c f_- \bar{u}_\nu (\gamma^5 - 1) m_1 v_1$$

and the entire matrix element M can be written in terms of f_+ and ξ:

$$M = \frac{G_F}{\sqrt{2}} \sin\theta_c f_+ [(p_K + p_\pi)^\lambda \bar{u}_\nu \gamma_\lambda (1+\gamma^5) v_1 + \xi m_1 \bar{u}_\nu (\gamma^5 - 1) v_1]$$

In this form we see that all ξ dependence comes in the term proportional to m_1 and is thus negligible in K_{e3} decays. In principle, we can determine f_+ from K_{e3} and then f_- from $K_{\mu 3}$ decays. Experimentally, this is quite difficult and the exact forms of f_+ and f_- are still not well known. We note that since there is only one significant amplitude in K_{e3} decays, in this approximation there is no possibility of interference and thus no CP violation in these decays.

Since the momentum transfer q^2 varies in $K_{\mu 3}$ decays only over the range $0.6 m_\pi^2$ to $(m_K - m_\pi)^2 = 7.2 m_\pi^2$, we can use a linear parametrization of the form factors. A conventional choice is[16]

$$f_\pm(q^2) = f_\pm(0)[1 + \lambda_\pm q^2/m_\pi^2]$$

$$f_o(q^2) = f_+(q^2) + [q^2/(m_K^2 - m_\pi^2)] f_-(q^2)$$

or

$$f_o(q^2)=f_o(0)[1+\lambda_o q^2/m_\pi^2]$$

with f_- constant (i.e. $\lambda_-=0$), which agrees with the data.

Most experiments measure the set of parameters λ_+,λ_o. We can define ξ in terms of λ_+ and λ_o as

$$\xi(0)=(\lambda_o-\lambda_+)(m_K^2-m_\pi^2)/m_\pi^2$$

$$\xi(q^2)=\xi(0)/(1+q^2/m_\pi^2)$$

Current values for these parameters for $K^+_{\mu 3}$ are[2]:

$\lambda_+=0.026\pm0.008$ and

$\lambda_o=-0.003\pm0.007$, thus Re $\xi(0)=-0.35\pm0.14$.

Previous measurements of Im ξ give $\mathrm{Im}\xi(0)=-0.09\pm0.21$[17]. For $K^o_{\mu 3}$, $\mathrm{Im}\xi(0)=0.009\pm0.030$[18].

Because of the definite helicity of the massless neutrino emitted in $K_{\mu 3}$ decay, the muon is completely polarized, in a direction which is determined by $\xi(q^2)$. The muon polarization as a function of $\xi(q^2)$ has been calculated by MacDowell[19], by Cabibbo and Maksymowicz[20], and by Okun' and Khriplovich[21]. In the laboratory frame, we have:

$$\hat{S}_\mu^{LAB}=\vec{B}/|\vec{B}|$$

and

$$\vec{B} = b_1(\xi)\{(\frac{\vec{p}_\mu}{m_\mu})[\frac{\vec{p}_\nu\cdot\vec{p}_\mu}{E_\mu+m_\mu}-E_\nu]+\vec{p}_\nu\}$$

$$+b_2(\xi)\{(\frac{\vec{p}_\mu}{m_\mu})[\frac{\vec{p}_K\cdot\vec{p}_\mu}{E_\mu+m_\mu}-E_K]+\vec{p}_K\}$$

$$-\mathrm{Im}\xi\{E_K(\vec{p}_\mu x\vec{p}_\pi)+E_\mu(\vec{p}_\pi x\vec{p}_K)+E_\pi(\vec{p}_K x\vec{p}_\mu)+[\frac{\vec{p}_\mu\cdot(\vec{p}_K x\vec{p}_\pi)}{E_\mu+m_\mu}]\vec{p}_\mu\}$$

where $b_1(\xi) = m_K^2 + m_\mu^2|b(q^2)|^2 + 2(\text{Re } b(q^2))(p_\mu \cdot p_k)$

$$b_2(\xi) = -2(p_\nu \cdot p_K) - (\text{Re } b(q^2))(q^2 - m_\mu^2)$$

$$b(q^2) = \frac{1}{2}[\xi(q^2) - 1]$$

with $p_a \cdot p_b = E_a E_b - \vec{p}_a \cdot \vec{p}_b$

The formula for the kaon rest frame is obtained by setting $\vec{p}_K = 0$ and $E_K = m_K$. In this frame the term proportional to Imξ, the CP violating part of the form factors, reduces to $m_K(\vec{p}_\mu \times \vec{p}_\pi)$, and thus a vanishing Imξ, implying time reversal invariance, requires a zero polarization P_n normal to the decay plane.

The form factor pair $f_o(q^2)$ and $f_+(q^2)$, defined above, define the amplitudes for the $K_{\mu 3}$ decay for the two possible spin-parities of the lepton pair (1^- and 0^+ respectively). The ratio of the amplitudes for the two transitions is thus a function of $\xi(q^2)$:

$$\frac{f_0(q^2)}{f_+(q^2)} = 1 + \frac{\xi(q^2) q^2}{m_K^2 - m_\pi^2}$$

Because the helicity of the massless neutrino is constrained, the 1^- and 0^+ transitions involve a muon helicity of +1 and −1, respectively. Thus in the kaon rest frame, one can describe $K_{\mu 3}$ decays in terms of the two amplitudes A_u, A_d representing the two muon helicities +1 and −1 respectively.

We can then write the components of the muon polarization in the following way:

$$P_t = 2\text{Re}(A_u^* A_d)/(A_u^2 + A_d^2)$$

$$P_n = 2\,\mathrm{Im}(A_u^* A_d)/(A_u^2 + A_d^2)$$

and the ratio

$$P_n/P_t = \mathrm{Im}(A_u^* A_d)/\mathrm{Re}(A_u^* A_d) = \tan\phi$$

with $A_u = |A_u| e^{i\phi}$ and choosing A_d real. The angle ϕ we have obtained is the complex phase between the two interfering amplitudes and is thus another way of expressing the violation of CP invariance. By using the formula given above for the muon polarization, and working in the kaon rest frame, one can derive the following relation between ϕ and Im ξ:

$$\tan\phi = \left(\frac{P_n}{P_t}\right)_{K_{CMS}} = \frac{-\beta_\mu \gamma_\mu \mathrm{Im}\xi}{m_K/m_\mu + \gamma_\mu(\mathrm{Re}\xi - 1) + (m_\mu/4m_K)|\xi - 1|^2}$$

with $\beta_\mu = |\vec{p}_\mu|/E_\mu$ and $\gamma_\mu = 1/(1-\beta_\mu^2)^{1/2}$

We have so far neglected any interactions between the final state particles. The coulomb interaction between the μ^+ and the π^- in $K^0_{\mu 3}$ decays leads to a polarization component in the direction P_n. With only one charged particle emitted in $K^+_{\mu 3}$ decays, the dominant interaction is between the μ^+ and the electric monopole moment (spherical charge distribution) of the π^0. The induced component P_n is thus orders of magnitude weaker in the $K^+_{\mu 3}$ system than in the $K^0_{\mu 3}$ decay. The final state interaction in $K^0_{\mu 3}$ is on the order of α, the fine structure constant, and is of the order of magnitude of the current experimental uncertainty in P_n in the $K^0_{\mu 3}$ system[18]. For $K^+_{\mu 3}$ decays, two different aspects of the final state interaction have been calculated. Zhitnitskii[22] has calculated the electromagnetic component of P_n to be approximately $0.1\alpha m_\mu/12\pi^2 m_K \approx 10^{-6}$, while Ginsberg[23] has found the pro-

portional radiative correction to the polarization P_n to be of order $\alpha/\pi=0.0023$, which is negligible.

A search for violation of CP invariance in $K_{\mu 3}$ decays was first suggested by Sakurai[24] in 1958. He pointed out that the triple cross product $\vec{s}_\mu \cdot (\vec{p}_\pi x \vec{p}_\mu)$, the muon polarization normal to the decay plane, is odd under T reversal and thus odd under CP reversal, by the CPT theorem. The triple cross product is also odd under C conjugation, thus even under CPT reversal. Since it is odd under C, the sign of a possible violation for $K^+_{\mu 3}$ and $K^-_{\mu 3}$ would be opposite. Sakurai also pointed out that in the case of $K^0_{\mu 3}$ a small CP violating polarization could be masked by an electromagnetic final state interaction.

The various CP violating theories yield different predictions for $K_{\mu 3}$ decays. In the Kobayashi-Maskawa model, CP violation is introduced in the quark mass matrix. Thus a theoretical prediction of f_+ and f_- would be expected to include a complex factor which would translate directly into $Im\xi$. In the Higgs models, a second term is added to the Lagrangian, corresponding to the decay s->u+H (Figure 1). This term contains a part complex relative to the part for the decay s->u+W, which contains the terms f_+ and f_-, both relatively real. The two terms can be combined into one, with an effective f_- which is complex relative to f_+ and thus gives an imaginary component to ξ[25].

We have seen already that in the Kobayashi-Maskawa model, CP violation occurs only when heavy quarks are involved. In $K_{\mu 3}$ decays, these heavy quarks appear only in second order, in loop diagrams. Thus the CP violating parameter $Im\xi$ can be expected to

be of order g^2, with g in the Kobayashi-Maskawa model = $G_F \sin\theta_2 \sin\theta_3 \sin\delta = 10^{-3} G_F = 10^{-8}$.

In the Higgs models, the term in the matrix element due to the Higgs interaction (Figure 1) is of the form

$$M_H = iG_F \sin\theta_c (v_2/v_3)^2 \frac{m_1 m_s}{m_o^2} \langle \pi^o | \bar{u}_L s_R | K^+ \rangle \bar{u}_\nu (\gamma^5 - 1) v_\mu$$

where m_1 is the muon (lepton) mass and v_2, v_3 are parameters related to the vacuum expectation values of the Higgs fields. We assume, with Zhitnitskii[22], that $(v_2/v_3)^2$ is of order unity. The bare Higgs mass m_o=2 GeV, and the term $\langle \pi^o | \bar{u}_L s_R | K+ \rangle \approx f_+ m_K^2 / 2\sqrt{2} m_s$.

The total matrix element is then

$$M = M_W + M_H = \frac{G_F}{\sqrt{2}} \sin\theta_c \{ f_+ (p_K + p_\pi)^\lambda \bar{u}_\nu \gamma_\lambda (1+\gamma^5) v_\mu$$

$$+ f_- m_1 \bar{u}_\nu (\gamma^5 - 1) v_\mu$$

$$+ i\sqrt{2} (v_2/v_3)^2 \frac{m_1 m_s}{m_o^2} \frac{f_+ m_K^2}{2\sqrt{2} m_s} \bar{u}_\nu (\gamma^5 - 1) v_\mu \}$$

We can combine the last two terms:[26]

$$\left[f_- + \frac{i}{2} \left(\frac{v_2}{v_3}\right)^2 f_+ \frac{m_K^2}{m_o^2} \right] m_1 \bar{u}_\nu (\gamma^5 - 1) v_\mu$$

$$= f_-^{eff} m_1 \bar{u}_\nu (\gamma^5 - 1) v_\mu$$

This gives us

$$\mathrm{Im}\xi = \mathrm{Im} \frac{f_-^{eff}}{f_+} = \frac{m_K^2}{2m_o^2} \left(\frac{v_2}{v_3}\right)^2 \approx \frac{0.1219 (\mathrm{GeV})^2}{m_o^2}$$

The polarization component normal to the decay plane, P_n, is of order

$$\frac{m_\mu m_K}{2\sqrt{2}m_o^2}\left(\frac{v_2}{v_3}\right)^2 = \frac{m_\mu}{\sqrt{2}m_K}\mathrm{Im}\xi = 4.61\times10^{-3}\left(\frac{v_2}{v_3}\right)^2$$

for m_o=2 GeV.

The CP violating polarization, P_n, is proportional to $m_\mu m_K/m_o^2$, so that a heavier Higgs mass would suppress the size of the CP violation. For the more general particle decay P_{13}, the preceding argument carries through, and we find a larger P_n for a heavier lepton or quark participant in the decay. For example, decays such as $D_{\mu 3}$ may be expected to have a larger component P_n than expected for $K_{\mu 3}$.

On the other hand, in neutron beta decay we expect a much smaller CP violating effect because the mass of the electron and u quark are much less than that of the muon and s quark, respectively. The experimental limit on $P_n=\vec{\sigma}_n\cdot(\vec{p}_1 x\vec{p}_\nu)$ in neutron beta decay is[2] -0.0009 ± 0.0013, and for the nuclear beta decay of Ne^{19}, $P_n=\vec{J}\cdot(\vec{p}_1 x\vec{p}_\nu)$ has been measured[27] to be -0.0005 ± 0.0010. Both results are consistent with time reversal invariance.

C. Muon Decay

In the muon decay $\mu^+\to e^+\nu_\mu\nu_e$, measuring the direction of the positron emission allows the direction of the muon polarization to be determined. The matrix element for the decay is[15]:

$$M = \frac{G_F}{\sqrt{2}}\bar{u}_{\nu_e}\gamma^\lambda(1+\gamma^5)\nu_e\bar{\nu}_\mu\gamma_\lambda(1+\gamma^5)\nu_{\nu_\mu}$$

In the rest frame of the muon, with polarization $\vec{S}$, the distribution of the positron (with momentum $\vec{p}$) is:

$$\frac{d^4N}{d^3pdt} = \frac{1}{\tau}e^{-t/\tau}\,\frac{1}{4\pi}[2x^2(3-2x)][1+(\frac{2x-1}{3-2x})(\vec{S}\cdot\hat{p})]$$

with $\hat{p}=\vec{p}/|\vec{p}|$, $x=E/E^{max}$, $E^2=(\vec{p})^2+m_e^2$, $E^{max}\approx\frac{m_\mu}{2}$, $\tau=\frac{192\pi^3}{G_F^2 m_\mu^5}$ and $\cos\theta_{sp}=\vec{S}\cdot\hat{p}$

The decay probability is largest when the positron energy is large ($x\approx1$) and the direction of emission is along the polarization direction ($\theta_{sp}\approx0$).

In a magnetic field B, the muon polarization will precess about the field direction with the Larmor frequency $\omega=g_\mu e|\vec{B}|/2m_\mu c$. In terms of components of polarization parallel to and perpendicular to the field direction, we have

$$\vec{S}(t)=(\vec{S}(0)\cdot\hat{B})\hat{B} + (\vec{S}(0)x\hat{B})\sin\omega t + (\hat{B}x(\vec{S}(0)x\hat{B}))\cos\omega t$$

In the present experiment, the magnetic field is parallel to the detection counter and the intensity of observed muon decays is

$$I(t)=Ne^{-t/\tau}(1 + \alpha\cos(\omega t+\phi_0))$$

with N the number of muons whose decay positron is detected. The asymmetry parameter α equals $\eta|\vec{S}_\perp(0)|$, with η the analyzing power. The phase ϕ_0 is the initial aximuthal angle of the muon spin about the precession axis as measured from $\hat{n}$, the direction of the adjacent counter.

II. Experimental Apparatus

A. Introduction and Experimental Overview

In order to measure the CP violating muon polarization in $K_{\mu 3}$ decays, it was necessary to construct an experimental apparatus which could accomplish several different goals. We needed to create a beam of kaons, and detect the resultant $K_{\mu 3}$ decays, distinguishing these particular decays (with a branching ratio of 3.2%) from other kaon decays and the interactions of other particles in the beam line. This set of all $K_{\mu 3}$ decays contained certain decay configurations in which the CP violating polarization would be large and measureable in our apparatus. We needed to select these certain decays, defined by the energies of the produced particles in the center-of-mass system, from the set of all $K_{\mu 3}$ decays. For these good $K_{\mu 3}$ events, we needed to bring the muon to rest and measure its polarization by observing the direction of emission of the decay positron. We discuss briefly here the techniques we used to obtain these goals and then describe in detail each part of the apparatus. Figure 2 is a schematic of the experimental apparatus.

We required an intense source of kaons with a minimal amount of background, which we obtained with a specially designed beam line with a broad momentum acceptance and a large angular acceptance. The beam line was short enough that a large proportion of kaons survived passage through the magnet zone to decay in a drift space beyond the magnets. Quadrupole magnets were used to focus the beam so that the beam particles passed without in-

teraction through a hole in the center of each part of the apparatus.

We established a five meter section in this region following the magnets, and placed the rest of our apparatus after this decay zone. A toroidal magnet and energy degrader was placed at the end of the decay area to slow down and focus positive muons into a polarimeter, which measured the polarization of muons which stopped in it. Scintillation counter arrays were used to track the path of the muon through the apparatus, as part of the procedure used to select useful events.

The $K^+_{\mu 3}$ decay also creates a neutral pion which itself decays almost immediately into two gamma rays. For events selected by our apparatus, one of the gammas traveled close to the beam line, through the hole in the center of each apparatus, and was detected in a lead glass calorimeter placed at the end of the experimental area. The kinematics of the decay was such that the other gamma was not detected by the lead glass array, and thus we could make accurate energy measurements only on the one gamma entering the calorimeter. However, this enabled us to make an energy cut on events accepted, taking only those events with gammas with greater than a certain energy. This proved useful in making a careful measurement of the muon polarization, as we shall see below.

The energy of the beam line was chosen to be about 4 GeV. Monte Carlo simulations were used to calculate the performance of the experimental apparatus as various design parameters were varied. In particular, the event acceptance as a function of en-

ergy was studied, as was the sensitivity of the apparatus in measuring any CP violating polarization. A much higher energy would have resulted in a larger event acceptance, but those events selected would have had a much smaller sensitivity to a CP violating polarization. At lower energies, the sensitivity of the apparatus would have been larger, but the event acceptance would have been smaller.

A sophisticated electronics system was constructed to analyze the signals from the scintillation counters and the lead glass array. A trigger was built which essentially looked for a coincidence between a muon path through the apparatus and a gamma hit in the lead glass. The muon path requirement was a hit in the A or B arrays at the end of the decay zone, a hit in an M counter placed after the toroidal magnet and a hit in an F counter placed on the upstream side of the polarimeter. These hits were required to be in the same azimuthal section in each array, thus defining an acceptable muon trajectory. This pattern of hits determined that a muon entered the polarimeter. Other electronic circuits were used to monitor other counters which determined whether or not the muon stopped in the polarimeter, and if it did, in which direction the decay positron was observed. A summary of the information for each event was read into a computer, which performed an on-line data analysis and also wrote the relevant information on magnetic tape for off-line analysis. Using the on-line analysis, the accumulated measurements of the muon polarization (the fundamental experimental results) were available within seconds at any time during the experimental run.

We were seeking a CP (or T) violating component of muon polarization normal to the decay plane in the kaon rest frame. We designed the selection of events so as to accept events in which the kaon beam direction was nearly in the decay plane in the center of mass system. In the laboratory frame, the beam direction was also in the decay plane for these events. By selecting events in which the pion direction was along the beam line, we ensured that the T violating decay correlation $\vec{s}_\mu \cdot (\vec{p}_\pi \times \vec{p}_\mu)$, defined in the center-of-mass system, would be determined by measuring $\vec{s}_\mu \cdot (\vec{p}_K \times \vec{p}_\mu)$ in the laboratory frame.

Figure 3 shows two possible orientations of the products of the kaon decay. In the first class of events, the pion is moving with the kaon and the CP violating polarization of the muon can be taken to be out of the figure. In the second class, the pion is moving opposite to the boost direction and in the lab frame is moving forward with only a small momentum. In this case the CP violating polarization is into the figure, and thus has an opposite sign to that of the first case. The energy of the gamma from the pion decay which is detected in the first class is much larger than the gamma energy detected in the second class, and it was possible to design an energy cut which would only pass events of the first class. This avoided contamination of the CP violating polarization of the first class by that of the second class, which would be of opposite sign. The energy cut, (at 1.2 GeV for a 4 GeV beam) also served to eliminate spurious low-energy hits in the lead glass.

Although two gammas are produced by the pion decay, only

one was detected in our array. The two gammas are emitted back-to-back in the rest frame, and the kinematics of the $K_{\mu 3}$ decay are such that in the boost to the lab frame the opening angle between the two is always greater than 10 degrees. The lead glass array, on the other hand, subtended a maximum angle of 7 degrees as seen from the decay zone through the holes in the toroid and polarimeter. Thus only one gamma would be expected to be detected in the array, and the event selection was designed so that the only events selected were those with localized showers, in which only one section of the lead glass was hit. This eliminated spurious signals due to the coincidence of two or more separate showers whose total energy was more than 1.2 GeV.

The components of the muon polarization in the lab frame can be described in terms of three components P_l, P_t, and P_n which lie along mutually orthogonal axes. The longitudinal polarization P_l lies along the muon momentum, and the components P_t and P_n are the transverse components in and normal to the decay plane $(\vec{p}_K x \vec{p}_\mu)$ respectively. The toroidal magnet was designed to focus the muon so that it entered the polarimeter approximately parallel to the kaon beam line. Thus, if the muon stopped in the polarimeter, its polarization component P_t was radially normal to the beam axis while the CP violating component P_n was perpendicular to the plane containing both the muon and the beam axis.

The geometry of the polarimeter (Figure 4a) allowed both P_t and P_n to be analyzed. Each of the thirty-two aluminum wedges in the polarimeter was flanked by two counters, labeled here U and D, with both the wedges and the counters being distributed

radially about the beam axis. The muons stopped in the wedges in the polarimeter and their spins precessed in a 55 gauss magnetic field. We measured the detection asymmetry between the two counters U and D, A=(U-D)/(U+D), as a function of time. For an ensemble of muons, the asymmetry varies sinusoidally as a function of ωt, with $\omega/2\pi$ the precession frequency of 745 KHz. Figure 4b shows the contributions to A from P_t and P_n, the CP conserving and CP violating polarizations, respectively. The CP conserving polarization P_t varies as $\sin\omega t$ while the CP violating component P_n varies as $\cos\omega t$. Thus by reversing the magnetic field each pulse and thus changing the sign of ω, it was possible to isolate the relatively small component P_n from the predominant component of the asymmetry P_t.

B. Beam Line

A specially designed beam line (Figure 5) was used to create a 4 GeV positively charged beam which entered the experimental area. The beam was designed with a broad momentum and angular acceptance in order to produce an intense source of kaons with a minimal amount of background. The beam line consisted of four magnets (two bending dipoles and two focussing quadrupoles), each with a specially prepared collimator.

The initial proton beam (energy 29.2 GeV), focussed on a platinum target located just in front of the beam line, produced particles over a broad range of momenta and angle. The selection of a specific momentum was accomplished by a large bending magnet with a specially constructed curved collimator in the magnet

channel. A 22 kilogauss magnetic field in the 1.82 meter (72 inch) long magnet selected the beam energy by bending 4 GeV kaons by eighteen degrees over the magnet's length. This 18^{o} bend was matched by the main channel of the brass collimator, so that particles with energy much different from 4 GeV interacted with the collimator. A second channel in the collimator went essentially straight through and carried the impacting 29.2 GeV beam into a beam dump made of heavi-met. The exit channel was 3.8 cm wide by 13.97 cm high (1.5 by 5.5 inches) and the momentum resolution was 10%, full width at half maximum(FWHM).

Two focussing magnets, each 0.81 meters (32 inches) long, were used to focus the beam so that it would travel through beam holes placed in the center of the various detectors without interacting with material. The two focussing magnets were placed between the two bending magnets.

The second bending magnet reduced the chromatic aberration of the beam by focussing the various momenta all at one point. The target (the object in this beam optics) was a platinum slab 10.2 cm long (about one interaction length) and 7.6 by 10.2 mm in cross-section. The image of the target was located 16.25 meters (640 inches) downstream and was 3.81 cm wide by 15.24 cm high (1.5 by 6 inches). At the image, the lead glass array was placed, with a center hole 22.86 cm high and 5.72 cm wide (9 by 2.25 inches). The second bending magnet, which was 0.91 meters (36 inches) long, also served to shield the beam line from the primary interaction region.

To reduce the halo from the beam, poured lead collimators

were placed in the two focussing magnets, in the second dipole, and in the 1.5 meter space following the last magnet. The size of these collimators, as well as the optics of the beam line, are indicated in Figure 6.

A concete collimator, hollowed out in the shape of a cone, 15.24 cm (6 inches) in diameter at the upstream end and 0.66 meters (26 inches) in diameter at the downstream end, followed the last magnet. The conical section was 1.75 meters long and was preceded by a 7.62 cm (3 inch) long cylindrical section 15.24 cm in diameter. This cone was filled with helium and the first 0.5 meters of the collimator were packed with paraffin (for neutron absorption) to leave a 10.16 cm (4 inch) wide by 7.62 cm high passage. After passing through the cone the beam entered the experimental cave, and travelled through the apparatus inside a helium-filled bag (to minimize scattering) to a beam dump, which consisted of a lead and uranium plug at the end of the experimental cave. The beam dump was surrounded by blocks of paraffin and boron to slow down and absorb neutrons produced in the dump by the interactions of the 4 GeV beam particles.

The acceptance of this beam line was 1.5×10^{-4} GeV-steradian, and the momentum resolution was 400 MeV, FWHM. By adjusting the strengths of the various magnets, slightly different beam energies could be obtained. For a typical proton intensity of 4.3×10^{10} incident on target per pulse, the calculated flux from this beam line acceptance, consistent with experimental measurements, was 3.6×10^{6} kaons, 4.3×10^{7} pions, and 2.2×10^{7} protons.

C. Decay Zone

Our apparatus was designed to accept kaon decays which took place only within a certain decay zone, which was located downstream of the magnets and upstream of most of the detectors. At the end of the decay zone two concentric arrays of scintillation counters (the A and B arrays) were placed, and one requirement for an acceptable event was a muon passing through one of the two arrays.

The five-meter long decay zone (Figure 7) began at the upstream end of the concrete cone collimator, 7.63 meters downstream of the target. An array of 8 counters(V) was located on the downstream face of the cone, approximately in the middle of the decay zone. This V array determined where in the decay zone the decay had taken place, and the A and B counters differentiated between large and small muon transverse momentum. Thus we were able to distinguish four types of events: A-V, B-V, A with no V, and B with no V, and compare the observed rates with the Monte Carlo calculations.

Three sets of anticoincidence counters were also placed in the decay zone. The 4 AC counters were placed at the beginning of the decay zone, the 6 K counters were placed at the position of the V array but at a larger radius from the beam line, and the 8 C counters were positioned between the beam line and the B array, at the end of the decay zone. The AC, K, and C arrays were all part of the trigger veto.

The A and B hodoscopes at the end of the decay zone con-

sisted of an outer ring (A) of sixteen counters, with outer diameter 0.574 meters and inner diameter 0.337 meters, and an inner ring, the B array (8 counters), with outer diameter 0.366 meters and inner diameter 0.186 meters. These arrays were centered symmetrically on the beam line to ± 1 mm and were perpendicular to the beam line to ± 10 mr. Furthermore, we measured no relative rotation between the two arrays to within 2 mr. Such a relative rotation, forming a screw sense in the apparatus, might have introduced a spurious CP violating signal. Positioning the arrays to the accuracy noted ensured that any such induced component would be negligible in this experiment.

D. Toroidal Magnet

A toroidal magnet placed following the A and B hodoscopes was designed to focus positive muons into the polarimeter while degrading their energy so that they would be more likely to stop in the polarimeter. This dual function was accomplished by making a toroidal core which increased in axial thickness with radius, and a complementary section which was used to maintain equal path length through the material for all muons.

The toroidal core was wound with 704 turns of AWG #12 copper wire. The complementary plug was placed immediately downstream of the magnet core, and both pieces were constructed from 17.8 cm (7 inch) thick machined laminations of 1010 steel. The magnet core was wound with constant pitch, but with half the turns applied clockwise about the toroid axis and half applied counterclockwise, in order not to introduce an axial component to

the magnetic field, which would have introduced a screw sense to the focussing effect of the toroid.

A current of 13 amperes produced an average saturated magnetic field of 15 kilogauss in the toroid. The cylindrical toroid was 71 cm (28 inches) long, with an inner radius of 17.8 cm (7 inches), allowing the beam to pass through the toroid, and an outer radius of 61 cm (24 inches). The mass of the toroidal assembly was 6000 kg, representing 560 g/cm^2 of steel, and this mass served to shield the polarimeter from background.

The M array of eight counters was mounted on the downstream face of the toroid. In conjunction with the F counters, mounted on the upstream side of the polarimeter, these counters helped determine the muon path. A piece of steel 5.08 cm (2 inches) thick was placed between the M and F counters. This steel absorbed soft particles which left the toroid, and converted photons into charged particles, which could be vetoed by guard counters, thus reducing the background in the polarimeter.

E. Polarimeter

A polarimeter, placed following the toroidal magnet, was used to stop the muons and determine their polarization. Counters were mounted on the various faces of the polarimeter and inside it as well, to track the muons as they came to rest and to detect the positron emitted in the muon decay. Muons with an initial laboratory kinetic energy of greater than around 1265 MeV passed through the polarimeter, while the mass of the toroid stopped muons with energy less than around 825 MeV, defining the

energy range of muons accepted by the polarimeter.

The magnetic field throughout the polarimeter had to be uniform, so that wherever the muon stopped, it experienced the same precessing field. A strictly axial field was required to avoid mixing the muon polarization components P_l, P_t, and P_n. Such a mixing would have diluted our measurement of the CP violating component P_n. The axial field was achieved by placing a steel plate on each end of the polarimeter to act as a mirror to the magnetic field, and by careful winding of the solenoidal coil. The direction of the magnetic field was reversed each pulse in order to eliminate any systematic asymmetry in the polarimeter's detection efficiency. The axial field in the two directions was measured to have the same magnitude to within 30 milligauss. Such a small difference introduced no error in our measurements.

Thirty-two wedge-shaped aluminum blocks set concentrically about a 36.83 cm (14.5 inch) diameter 9.5 mm thick stainless steel beam pipe made up the heart of the polarimeter. Two 3.2 mm (1/8 inch) thick scintillation counters(G) were placed in slots located between each pair of wedges. The coincidence of each pair in a slot was required in all the electronic logic dealing with the G counters. The requirement of a hit in both thin counters, which demanded a minimum energy deposit of 1/2 MeV in each counter, helped to eliminate background from neutrons and low energy photons.

To further reduce background, each wedge was surrounded by scintillation counters logically placed in anti-coincidence to

the G counters. These counters detected particles passing through the wedge which might have been mistaken for muon decays. The F and I counters were mounted on the upstream and downstream face of each wedge, and a set of four curved counters(P) were placed inside the beam pipe. The P counters were covered on the inner radius (facing the beam) with 6.4 mm (1/4 inch) of lead, to convert photons. Four small sickle shaped counters(P') were mounted on the front face directly around the beam pipe, and shielded a small section of the wedges not covered by the F or P counters.

The track of the entering muon was determined by the prompt signals (associated with the trigger) in the counters in the polarimeter. Counters on the downstream face of the toroid(H) determined the octant in which the muon left the toroid. The trigger logic was designed so that this information had to agree with the F signal, which indicated which of the thirty-two wedges the muon entered. A prompt signal in an adjacent G counter (or counters) indicated multiple scattering of the muon from one wedge to another. The electronics used to process an event used the information recorded by latch modules (triggered by the prompt trigger) to determine in which wedge, if any, the muon had stopped.

The thirty-two wedges in the polarimeter were cast from #356 No Heat Aluminum and were 91.4 cm long. The outer radius was 53.3 cm and the inner radius 40.6 cm. Each had a mass of 47 kg representing 250 g/cm^2 of aluminum. Each wedge was carefully machined to be symmetric.

A solenoidal coil (diameter 1.25 m) was wound around the

wedges on a plastic coil form. This coil consisted of 482 turns of 3.2 mm x 3.2 mm copper wire which were wound in two layers with opposite pitch, and with an equal number of turns in each layer, in order to preserve the axial nature of the field. A coil current of ten amperes through the coil created an axial field of 55 gauss which was measured to be uniform over the active volume to within 1%. Between beam pulses the field direction was reversed, as noted above, and the relaxation time constant for the system was 0.08 seconds. Since the beam spill was one second long every 3 seconds, the magnitude of the field was constant during the beam pulse.

The entire polarimeter, except for the beam pipe, was surrounded by a shell of 1010 steel which was formed by a 6.4 mm thick cylinder capped on both ends with a 12.7 mm thick plate. This shell, on which the F, I, and P' counters were mounted, acted as a magnetic shield from stray external fields and also as a return plate for the solenoid's own field, and thus maintained the axial nature of the field.

The 2500 kg polarimeter was mounted so that it could be rotated about its axis (the beam line), so that studies could be made of subtle systematic effects.

F. Lead Glass Array

A lead glass calorimeter, used to detect and measure the energy of a gamma ray from the pion decay, was placed downstream of the polarimeter, at the focus of the charged beam line. The calorimeter consisted of an array of 48 lead glass blocks, and

the signal in each piece, which was proportional to the energy deposited in that counter, was added together by a part of the trigger electronics, thus determining the total energy deposited in the whole array.

The energy of the incident gammas was measured by detecting the Cerenkov light produced by the resultant shower. The Cerenkov light produced by an electromagnetic shower in a lead glass counter is linearly proportional to the energy of the incident particle. We measured the energy resolution of these pieces of glass to be $15\%/\sqrt{E}$(in GeV) over the energy interval we were interested in (one to three GeV). We were only interested in the energy deposited by neutral particles and so four scintillation counters(D) placed in front of the lead glass array were set in anticoincidence to the calorimeter input to the trigger, in order to veto incoming charged particles.

The calorimeter was designed to accept gamma rays produced at a wide enough angle from the beam line to be distinguishable from the particles in the beam, but at a small enough angle to pass through the center hole in the polarimeter. The dimensions of the array are indicated in Figure 8. A hole for the beam to travel through was left in the center of the array, and the outer dimensions were determined by the 36.83 cm (14.5 inch) beam hole in the center of the polarimeter. The non-symmetric hole in the lead glass array was designed to fit the image of the target generated by the highly astigmatic lens system. The bricks were composed of Schott SF5 lead glass and were 25.4 cm (10 inches) long (about ten radiation lengths).

Two identical signals were sent out from the base attached to the lead glass counter phototube (RCA 8575). One signal was sent to a discriminator which was then connected to a latch module, and the other went directly to an analog adder (LeCroy 127FL). The analog adder determined the size of the total energy deposit in the array, while the pattern of glass hits, as recorded by the latch module, were examined by the computer. The software program which collected the data discarded would-be events in which two different sections of the array were hit, implying two separate particles causing showers in the lead glass array.

The blocks were calibrated regularly through the run by measuring the charge deposited by straight-through muons which deposited in the calorimeter an amount of energy equivalent to that of 340 MeV electrons. Voltages for the phototubes were supplied by a remotely programmable high voltage supply (LeCroy HV4032) and were adjusted to keep the muon calibration charge constant.

The size of the signals from the lead glass counters was found to be very sensitive to the strength of the local magnetic field, since the photomultiplier tube gain varied sharply with the external magnetic field. Since the lead glass calorimeter was placed just downstream of the 55 gauss polarimeter solenoid, the field of which was reversed for each pulse, the solenoidal magnetic field had a noticeable effect on the reproducability of the lead glass measurements. We shielded the calorimeter by building a box made of pairs of 1.27 mm steel plates around the array.

This magnetic shielding reduced the effect of the solenoid by 50%. The residual effect did not seriously compromise the measurements.

G. Electronics and Data Handling

Three levels of data handling were designed for this experiment. A fast trigger signal was created for each coincidence of a muon in the polarimeter and gamma in the lead glass. Then a hardware data acquisition system looked at the event in more detail and passed on good events, in the desired format, to a small PDP-11 computer, which performed an on-line analysis and also wrote tapes, for off-line analysis. Figure 9 is a schematic of the fast trigger and FASTBUS electronics.

We used NE102 scintillator and RCA 8575 and Amperex 2312 phototubes on our scintillation counters. The phototube signals were converted into standard digital signals by LeCroy NIM discriminators. Typical widths of the signals from the discriminators were ten nanoseconds for counters involved in the trigger, box, and clock units and twenty nanoseconds for counters used only in anticoincidence. A set of signals from one hodoscope array, and the output from the lead glass analog adder, were specially prepared with 4 nanosecond widths and used as described below to give the trigger a 4 nanosecond resolution time. The output of the discriminators of the pair of G counters in each of the thirty-two slots in the polarimeter were placed in coincidence by NIM coincidence units, so that in all subsequent electronics, the G counters were treated as only thirty-two counters,

one in each slot.

An analog adder was used to measure the energy deposited in the lead glass array. The analog sum was received by a NIM discriminator which was set to trigger only on inputs which corresponded to energies greater than 1.2 GeV. An electronic trigger circuit[18], which determined that a muon had entered the polarimeter, also received the information from the NIM discriminator concerning the energy deposit in the calorimeter. Any coincidence of the muon in the polarimeter and an energy deposit (signifying a gamma ray with energy greater than 1.2 GeV) created a trigger signal which was passed to several components of the FASTBUS system (described below). The resolution time of the trigger, which was built using Emitter Coupled Logic (ECL) chips, was 10 nanoseconds. While the FASTBUS system was processing an event, possible triggers were inhibited so that the entire system was processing only one event at a time. This dead time was about 7 microseconds, with the bulk of this interval representing the 6.4 microsecond period for which the gate for muon decays was open.

Each of the hodoscope arrays was segmented azimuthally, and the muon section of the trigger looked for a coincidence between counters in the same azimuthal section of each array. This detailed coincidence helped ensure that the trigger signal represented an actual $K_{\mu 3}$ decay and not the coincidence of several different particles entering different parts of the apparatus at the same time. A hit in an A or B counter was correlated with a coincidence between one of the 8 M counters and one

of the 32 F counters.

Several hodoscope arrays were set in anticoincidence to the trigger. These counters recorded particles entering the experimental area which did not pass through the beam line and thus represented background particles scattering in the collimation region and which were not related to Kμ3 decays. Another veto on the trigger ensured that only one particle passed through the A and B arrays during the trigger resolution time. These vetoes reduced the chances that two different particles coincided to form the muon part of the trigger, one in the polarimeter and one in the hodoscopes.

A tight timing coincidence, with a resolution time of four nanoseconds, was created with NIM logic modules. This circuitry, which looked for the coincidence of an energy deposit greater than 1.2 GeV and a particle passing through an M counter (located on the downstream side of the toroid), was designed to supplement the fast trigger previously described. While the trigger looked for the detailed coincidence between many counters and thus had a large resolution time, the tight timing circuitry looked only for a simple coincidence and thus could be designed with a much smaller resolution time. However, this tight timing coincidence required a longer real time than the trigger electronics needed, due to the additional processing required for both the lead glass and M counter signals in order to reduce each signal's width to 4 nanoseconds. If the tight timing coincidence was not satisfied, the trigger signal was aborted.

The trigger signal was used by the FASTBUS data acquisi-

tion system as an initializing sgnal for the proccssing of an event. The FASTBUS system[28] is dcsigned to replace the CAMAC system as a general computer interfacc data handling system. This experiment marked the first time FASTBUS components were assembled and used for an experiment. Our implementation of FASTBUS included a water-cooled crate which could hold twenty modules and ECL electronics throughout, including an ECL level backplane. The FASTBUS system was connected to a PDP-11/20 computer via a special host interface module which resided in both the FASTBUS crate and the computer. The two sections were connected via a thirty-connector ribbon cable.

The bottom portion of figure 9 indicates the data processing sequence on the FASTBUS system. The FASTBUS modules received the fast trigger signal as well as the discriminated outputs of the various counter arrays. Six 32 channel coincidence modules were used to latch the information in the hodoscope counters at the time of the trigger.

A controller module[29] analyzed the latched counters and determined, using a special "boxfinder" module, in which aluminum wedge or "box" the muon had stopped. If the event was not aborted by the tight timing coincidence circuit or the controller's own analysis of the event, the controllcr next interrogated a 32 channel clock module, a Time-to-Digital Converter (TDC), which determined the time of the muon decay. Each channel of the TDC would time out aftcr 6.4 microseconds unless a muon decay (clock hit) was observed in the G counter corresponding to that channel. Each tick of the TDC clock was 100 nanoseconds, and the two chan-

nels on each side of the wedge were read for each event. The various guard counters placed around the polarimeter wedge (the F and P counters) were placed in anticoincidence to the clock hits, as was a special circuit which was activated only by the coincidence of three or more G counters. This last part of the veto was used to eliminate showers originating inside the polarimeter.

Events that successfully passed the hardware cuts were placed into a memory module, also on FASTBUS, which operated in a First In First Out mode, and which could be read asynchronously by the computer. The computer also read the scalers on the FASTBUS which were used to monitor the rates in the various counter arrays. The information placed into memory consisted of the pattern of the hodoscope, polarimeter, and lead glass counters latched, the calculation by the trigger of the event type (A, B, A-V, B-V), the box and decay time, and the direction of the solenoid field, which was obtained from a timing and I/O module.

The computer was used for software cuts on the data, on-line data analysis, and to write data tapes for later analysis. The data tapes consisted of the information read from the FASTBUS organized on a pulse by pulse basis. The software cuts and refinements included the following:

1) The rejection of events with either no clock stops or two clock stops, thus providing an unambiguous decay time and direction.

2) The rejection of events in which the pattern of latch hits in the lead glass indicated two or more particles hitting at the

same time. We required 1.2 GeV to be deposited from one and only one gamma.

3) Recalculation of the event type based on the latch hits. For the A-V and B-V types, we required the V counter hit to be in the same or nearby octant to the A or B counter. If the V counter was not adjacent to the A or B counter, the event was classified as type A or B. Furthermore, we required the A or B to be adjacent to the F octant. If two or more A or B counters were latched, the program selected the counter closest to the downstream octant hit and assigned the event the appropriate type.

The computer program running the experiment would read out the contents of the memory module, perform the above cuts on the events it received from the FASTBUS, write the information from each event on magnetic tape, and incorporate the pertinent information from each event into the on-line data summary which consisted of two parts. The short-term part consisted of scaler rates, latch hit distributions, clock and box stop information and was maintained up to 20,000 events. At this time, this information would be printed out for reference and the short-term summary was purged. This gave us information on the experimental conditions over short time scales (one to two hours). The long-term data summary consisted of the accumulated muon decay time statistics and the resulting asymmetries as a function of time for the total number of events and for each of the four types. This file was updated every 2,500 events and could be queried while data was being taken. Thus at any time we could obtain the accumulated CP violating and CP conserving polarization in only a few seconds.

III. Data Analysis

A. General

The data analyzed below consists of 20.8×10^6 events collected during 1500 hours of accelerator running time. With an incident proton beam of 4.3×10^{10} protons per second the calculated kaon flux was 3.6×10^6 per second, of which 5.8×10^5 kaons decayed per second in the five meter decay space. Typically, the pulse rate was 1 per 3 seconds, with a nominal pulse length of 1 second. Of the 18500 resultant $K_{\mu 3}$ decays, about 36 satisfied the various trigger requirements and produced a muon decay. In 1/3 of the muon decays we could detect the positron and thus determine the direction of polarization of the muon. Over the course of the experiment we averaged 12 such good events per pulse. The event rate was limited by accidental backgrounds rates, which, in turn, depended strongly on the time structure of the beam. The time structure, which was monitored continuously using special coincidence counters, varied with the operation of the accelerator. Under the most favorable accelerator running conditions we recorded more than 20 events per pulse.

Monte Carlo calculations were used to compare the relative distributions and polarizations of the various event configurations. The event acceptance of the apparatus was determined by propagating the muons and gammas from the kaon decays in the beam line through the entire apparatus, including in the calculations the energy-selected beam line, the trigger logic, and the geometry of the apparatus. Scattering processes in the toroid-

degrader and polarimeter which resulted in an effective depolarization were also included in the simulation. The muon polarization was calculated in laboratory coordinates using the Cabibbo-Maksymowicz[20] formula, with $\xi=0.0+0.01i$. Because our fundamental result was the ratio of the two polarizations, even very large uncertainties in the acceptance calculations do not significantly affect our conclusions.

Although the muon spin direction generally followed the muon momentum when moving in the toroidal magnetic field, nuclear coulomb collisions resulted in a depolarization[30] of about 5%. Multiple scattering in the toroid caused an additional 5% depolarization. Muons stopping in the polarimeter entered with an energy less than 500 MeV and suffered no additional depolarization as they came to rest in the aluminum wedges of the polarimeter[31].

These depolarizing effects do not create a false T violating signal, but rather decrease the sensitivity of the polarimeter. The analyzing power of the polarimeter was determined to be $\eta=0.11\pm0.02$, based on an analysis of the actual polarizations, measured under running conditions such that the accidental backgrounds were small, as compared with the Monte Carlo calculations.

We present the Monte Carlo results in Table 1. The four types A, B, AV, BV are based on the geometry of the muon hodoscopes in the decay zone (figure 7), with AV and BV types having occurred earlier in the decay zone and A and B types later in the region. We list the expected percentage of each type, and the expected components of polarization P_t and P_n, as calculated in the

kaon rest frame and in the laboratory frame. The laboratory sensitivity is less than the sensitivity in the rest frame of the kaon due to the depolarizing effects in the detector. At low backgrounds rates (and small number of good events per pulse), the measured intensities agree well with the predicted intensities. Most of the time we ran at higher beam intensities in order to obtain a larger event rate. In this configuration, the various types were subject to different amounts of background, and so the actual intensities diverge somewhat from the Monte Carlo predictions.

B. Muon Decay and Muon Asymmetry

To measure the polarization of muons stopped in a wedge of the polarimeter, we detected the positrons from the muon decay in counters placed between the wedges in which the muon stopped. The signals from these counters were used in the FASTBUS electronics to stop clocks associated with each channel. The clocks were started by the trigger circuitry, as described previously, and counted to 6.4 microseconds (in 0.1 microsecond bins) while waiting for a decay. The clocks could also be stopped by ionizing particles from various background sources such as neutrons, gamma rays, and charged particles. Although a clock veto was constructed using the counters which surrounded each wedge, not all backgrounds could be intercepted. Considering both valid muon clock stops and the random background, the time distribution of clock stops can be written as:

$$I(t) = e^{-\gamma_B t}(N^+ e^{-t/\tau^+} + B)$$

with N^+ and B the normalized amplitudes for the μ^+ and background levels, τ^+ the muon lifetime (2.198 microseconds), and γ_B the background decay constant.

Using a least squares fit to all the data, with the above formula and with the FUMILI[32] fitting routine, we find that the clock hits consisted of 75% μ^+ decays and 25% background for the sum of all running during the experiment. These random backgrounds were a major limiting factor in the rate of data collection and are discussed in detail in the next section.

The measured asymmetry in detection of the positron from muon decay, A= (U+D)/(U-D), was used to determine the transverse and normal components of the muon polarization. The cylindrical symmetry of the detector allowed us to combine the data from all 32 polarimeter sections. We define U as the intensity of positrons detected by the counter located on the clockwise side, looking downstream, of any polarimeter wedge; D is the corresponding quantity on the counter-clockwise side. The + and - subscripts indicate the direction of the axial field in the polarimeter and thus the direction of muon spin precession, with + indicating the field directed upstream, with the spin of the μ^+ precessing clockwise about the beam axis.

Combining the intensity distribution with the background parametrization, we obtain

$$U_{\pm}(t) = e^{-\gamma_B t}\{N^+[1 + a\cos(\pm\omega t + \phi)]e^{-t/\tau^+} + B\}$$

$$D_{\pm}(t)=e^{-\gamma_B t}\{N^{+}[1 + \alpha\cos(\pm\omega t + \phi)]e^{-t/\tau^{+}}+B\}$$

with ϕ the initial azimuthal angle about the beam axis of the muon spin, as measured from the outbound unit vector normal to the detector, and ω the precession frequency $=g_{\mu}eB/2mc$.

The T conserving transverse polarization is initially parallel to the plane which bisects the polarimeter block (see figure 10), so that $\phi\approx\pm\pi/2$, (+ for the D, - for the U counter).

The T conserving asymmetry is then

$$A_t(t) = \frac{(U_+-D_+)-(U_-D_-)}{U_++D_++U_-+D_-} = [A_t(0)/C(t)]\sin\omega t$$

where $C(t)=1+(B/N^{+})e^{t/\tau^{+}}$ and $A_t(o)=\eta P_t$, η the analyzing power.

For the T violating, normal component of polarization, $\phi\approx 0$ for the U counter and π for the D counter, and the T violating asymmetry is

$$A_n(t) = \frac{(U_+-D_+)+(U_-D_-)}{U_++D_++U_-+D_-} = [A_n(0)/C(t)]\cos\omega t$$

wit C as above and $A_n(0)=\eta P_n$. Note that $t=t_{meas}+t_o$, with t_o the instrumental phase shift. We can assume that the background contributions are symmetric for the U and D counters.

We plot the measured asymmetry A_t and A_n as a function of time, in figure 11. The T conserving asymmetry A_t clearly exhibits a sinusoidal form, with decreasing amplitude with time due to the background dilution, as expressed in the factor C(t). From a least squares fit to the entire event sample, we obtain $\omega/2\pi=745$ KHz and $t_o=0.018$ microseconds, consistent with measure-

ments made on the solenoidal field and clock electronics, respectively.

For the total event sample of 20.8×10^6 events, the fitted value for the asymmetry amplitude $A_t(0)=0.0753 \pm 0.0018$, and with analyzing power $\eta=0.11 \pm 0.02$ we obtain $P_t=0.685 \pm 0.125$, where the error follows largely from the uncertainty in the analyzing power of the polarimeter. This uncertainty does not contribute in an important manner to the uncertainty in the measurement of the CP violating polarization P_n.

The T violating asymmetry $A_n(0)=-0.00034 \pm 0.00058$, giving $P_n=-0.0031 \pm 0.0053$, consistent with zero and therefore time reversal invariance.

The resulting asymmetries for the four types are given in Table 2. The T violating asymmetry P_n is consistent with zero for each of the four types.

C. Backgrounds

The backgrounds in this experiment were of two different types:

1) False triggers, due principally to coincidences between unrelated muons and gammas.

2) Accidental counts in the polarimeter counters(G) which diluted the measurement of the muon polarization.

The trigger circuitry (described previously) was designed to accept $K_{\mu 3}$ decays and reject other events. The resolution time of the trigger, including the tight timing coincidence logic, was four nanoseconds. By requiring a coincidence between a muon fol-

lowing a well defined track and a gamma ray depositing more than 1.2 GeV into the lead glass calorimeter, we ruled out most random triggers. Subsequent electronics on the FASTBUS system checked that the muon had not left the polarimeter by passing through an I counter. Charged particles incident on the lead glass array were vetoed at the trigger stage by a set of scintillation counters covering the front face of the array. In addition, the software cuts included an examination of the hit pattern in the lead glass to ensure that the 1.2 GeV or greater deposited was due to only one electromagnetic shower. The trigger required an energy deposit greater than 1.2 GeV, thus discriminating strongly against straight-through charged particles which may have leaked through the anti-coincidence counters.

The other major K^+ decay modes are: $K^+ \to \mu^+ \nu_\mu$ (63.5% branching ratio), $\pi^+\pi^0$ (21.2%), $\pi^+\pi^0\pi^0$ (1.73%), $\pi^+\pi^+\pi^-$ (5.6%), $\pi^0 e^+ \nu_e$ (4.8%) and $\mu^+ \nu_\mu \gamma$ (0.53%). These could not mimic a $K^+_{\mu 3}$ decay in our apparatus, but a coincidence of a muon from $K_{\mu 2}$ and a gamma from one of the π decay modes could. Although the branching ratio for the radiative decay $K^+ \to \mu^+ \nu_\mu \gamma$ is 1/7 that for $K^+_{\mu 3}$, the gamma produced in $K^+ \to \mu^+ \nu_\mu \gamma$ is generally too low an energy to trigger a latch hit.

In a special test, we removed the requirement for a lead glass hit from the trigger logic, and determined that the trigger muon acceptance rate was 18,000 per pulse. We also measured that the rate for neutral particles entering the lead glass was 80,000 per pulse. The expected coincidence in the tight timing logic for these two rates was 5.7 events per pulse. As we only detected

the positron from muon decay in 1/3 of the events, this leaves us with 1.9 background events per pulse.

The number of events due to false triggers was thus less than 16%. These false events involve muons which are mostly longitudinally polarized, and so act only to decrease the effective sensitivity of the polarimeter. These backgrounds do not cause a false T violating signal.

The other major background problem was that of accidental counts in the polarimeter counters, mimicking a muon decay. Each of the polarimeter wedges was surrounded by guard counters which were used to veto apparent muon decays (clock stops) which were actually due to particles entering the polarimeter. The G counters, placed in the slots between the wedges, were used to detect the positron from the muon decay. A pair of counters was placed in each slot and a coincidence of the two counters was required for a hit in a "G counter". The coincidence rate for one such set of G counters, under normal running conditions, was about 50,000 per pulse. Charged particles entering the polarimeter accounted for 67% of these, and were removed by employing the veto counters mentioned above.

Those background hits in the muon counters which could not be removed by our anti-coincidence logic were due to a "neutral" flux. Part of this flux was "prompt", or related directly to the beam spill, and was believed to be due mostly to low energy photons scattering in the polarimeter. Shielding between the toroid and polarimeter was installed to try to reduce some of this background. Another part of the "neutral" flux was not

prompt and was believed to be due to thermal and evaporation neutrons entering the polarimeter. We attempted to remove some of this flux by placing paraffin and boron in front of the polarimeter to slow down the evaporation neutrons and absorb the thermal ones, but there was not enough space near the apparatus for the amount of these materials that would have been needed to appreciably reduce the noise. Many of the neutrons were believed to have been captured by Al^{27}, and the resultant gamma rays, as well as the gamma and beta rays emitted in the subsequent decay of Al^{28} (with half-life 2.3 minutes), were considered part of this "neutral" flux. These decays of Al^{28} were observed in our apparatus, and contributed about 4% to the muon counter background. Including the prompt gammas from the absorption of neutrons by Al^{27}, we find that about 15% of these backgrounds were caused by the capture in aluminum of thermal and epithermal neutrons.

D. Systematics

A spurious T violating effect could be produced in our apparatus only by an asymmetry defining a net screw sense in the detection of muon decays with respect to the laboratory kaon decay plane. We carefully constructed and mounted the apparatus to avoid such asymmetries, and thus reduced the systematic uncertainties to much less than the statistical uncertainties of the experiment.

The rotation of the transverse polarization P_t out of the decay plane, thus generating a component which would mimic a CP violating polarization P_n, could result from a screw sense pro-

duced by misalignments in the apparatus. The alignment of the various arrays was checked and the net angle of rotation found to be less than 2 milliradians. According to our Monte Carlo calculations, an angle of rotation θ would produce a component $P_n=0.10\theta P_t$, so for $\theta=2$ mr, $P_n=2\times10^{-4}P_t$, a negligible amount.

The reversing magnetic field used in the polarimeter avoided systematic errors due to possible asymmetries in the detection efficiency of the polarimeter. The axial field for the two polarities was required to be equal to avoid any screw sense generated by the direction of the current in the solenoid, and to avoid contamination of the CP violating polarization (which varied as $\cos\omega t$) by a term $P_t\cos(\omega t)\sin(\Delta\omega t)$, with $\Delta\omega$ the difference in the precession frequencies for the two directions. We measured the solenoidal fields in the slots in the polarimeter in which the counters were placed and determined that $\Delta\omega/\omega\leq5\times10^{-4}$, so that the contribution to P_n was less than 0.001.

The axial field also affected the efficiency of the lead glass counters. We measured the change between polarities of the field present at the position of the lead glass to be 1 gauss, and found an asymmetry of 5% in the number of events obtained in the two polarities, with an asymmetry of 10% in the number of lead glass counters hit. After placing shielding around the lead glass array, the change in magnetic field was reduced to 0.60 gauss, the event asymmetry to 4%, and the lead glass hit asymmetry to 3%. This type of asymmetry did not generate a screw sense, and the remaining asymmetry did not affect the accuracy of our measurements.

Other possible screw-sense asymmetries could be generated by the simultaneous linear displacements of two different arrays. For instance, if the A or B hodoscopes were displaced upward, causing (for instance) a 1% up-down asymmetry in the trigger, and if the polarimeter similarly displayed a 1% asymmetry in the horizontal direction, a maximum screw sense asymmetry of the order of 0.0001 could be generated. We monitored such asymmetries and the position of the arrays throughout the experiment to ensure that the contribution of such screw sense asymmetries was negligible.

IV. Conclusions

Using the asymmetry results for the entire running period (20.8 million events), we can deduce the limits set by this experiment on the violation of time reversal invariance in $K^+_{\mu 3}$ decays. The value of the T (or CP) violating component P_n was measured to be -0.0031 ± 0.0053. Monte Carlo calculations indicate that for $Im\xi=0.01$, $\langle P_n^{lab} \rangle = 0.00193$, so that the measured value of $Im\xi$ is -0.016 ± 0.027. The model for CP violation involving the Higgs bosons, discussed in Chapter 1, gives us $Im\xi = 0.0305(v_2/v_3)^2$, so we deduce that the Zhitnitskii parameter (v_2/v_3), which we expect to be of order unity, is less than 1.33, with a confidence level of 95%. The previous measurements[17] on $K^+_{\mu 3}$ give $Im\xi = -0.09 \pm 0.21$, and for $K^o_{\mu 3}$, where the final state interaction is not insignificant, $Im\xi = 0.009 \pm 0.030$[18].

We can also, more generally, describe the violation of time reversal invariance in terms of the complex phase which appears in the interference between two normalized amplitudes describing the decay, as discussed in Chapter I. In the neutron beta decay experiments cited earlier, the similar angle ϕ was found to be[3] $(0.11 \pm 0.17)^o$ for neutron beta decay, while for the Ne^{19} decay[17] $\phi = (-0.06 \pm 0.11)^o$. These values are to be compared with the value of 0^o expected if time reversal invariance is valid.

In $K_{\mu 3}$ decays, $\tan\phi = (P_n/P_t)_{K_{CMS}}$, as defined previously. From the Monte Carlo calculations, we obtain $\langle P_n^{lab} \rangle = 0.00193$, $\langle P_n^{CMS} \rangle = 0.00258$, and $\langle P_t^{CMS} \rangle = 0.655$. The measured value

$P_n = -0.0031 \pm 0.0053$, so that $\tan\phi = \phi = -0.0063 \pm 0.0103$. In the way expressed above for the neutron experiments, our result is $(-0.36 \pm 0.62)^\circ$. The $K_{\mu 3}$ experiment is more sensitive to possible CP violating effects than neutron experiments because of the heavy quark decay in $K_{\mu 3}$.

REFERENCES

1. J.Christenson, J.Cronin, V.Fitch, R.Turlay Phys.Rev. Lett.13,138(1964)

2. Particle Data Group(Barash-Schmidt et al.) Rev.Mod. Phys.52,S1(1980)

3. B.Winstein, in Proceedings of the Workshop on Nuclear and Particle Physics up to 31 GeV:New and Future Aspects, Los Alamos, edited by J.Bowman,L.Kisslinger,R.Silbar(Los Alamos,New Mexico,1981)

4. Some recent reviews on CP invariance violation include: J.Cronin, Rev.Mod.Phys.53,373(1981); S.Pakvasa, in High Energy Physics-1980, proceedings of the XX International Conference, Madison, Wisconsin, edited by L.Durand and L.Pondrom(AIP,New York,1981); L.Wolfenstein, in Particles and Fields-1979, proceedings of the Annual Meeting of the Division of Particles and Fields of the APS, Montreal, edited by B.Margolis and D.Stairs(AIP,New York,1980)

5. M.Kobayashi, T.Maskawa Prog.Theor.Phys.49,652(1973)

6. E.Shabalin, Yad.Fiz.32,443(1980) [Sov.J.Nucl.Phys.32,228 (1980)]

7. F.Gilman, M.Wise Phys.Rev.D20,2392(1979); B.Guberina, R.Peccei Nucl.Phys.B163,289(1980)

8. I.Altarev, et al., Phys.Lett.102B,13(1981)

9. P.Sikivie, Phys.Lett.65B,141(1976); A.Lahanas, C.Vayonakis Phys.Rev.D19,2158(1979)

10. S.Weinberg, Phys.Rev.Lett.37,657(1976); N.Deshpande, E.Ma Phys.Rev.D16,1583(1977); A.Ansel'm, D.D'Yakonov Nucl. Phys. B145,271 (1978); A.Ansel'm, N.Ural'tsev Yad.Fiz.30,465 (1979) [Sov.J.Nucl.Phys.30,240(1979)]; K.Shizuya, S.-H.Tye Phys.Rev. D23,1613(1981)

11. G.Branco, Phys.Rev.Lett.44,504(1980); G.Branco, Phys.Rev. D22,2901(1980)

12. I.Khriplovich, A.Zhitnitskii INP,Novisibirsk Preprint 81-07 (1981)

13. A.Sanda, Phys.Rev.D23,2647(1981); N.Deshpande, Phys. Rev. D23,2654 (1981); J.Donoghue, J.Hagelin, B.Holstein Harvard Univ. Preprint HUTP-81/A032(1981); J.Korner, D.McKay DESY Preprint 81/034(1981)

14. R.Mohapatra, J.Pati Phys.Rev.D11,566(1975); R.Mohapatra, G.Senjanovic Phys.Lett.79B,283(1978); J.Pati, A.Salam Phys. Rev. D10,275(1974); P.Cea, G.Fogli Istituto di Fisica,Bari Preprint (1981)

15. We use the convcntions of E.Commins, Weak Interactions (McGraw-Hill, New York,1973)

16. Ref.2, page S9. Also, L.Chounet, J.Gaillard, M.Gaillard Phys.Rep.4C,199(1972); J.Lemonne et al., Univ. of Brussels re-

port,1976 (unpublished)

17. A.Callahan, et al., Phys.Rev.150,1153(1966); D.Cutts, et al., Phys.Rev.Lett.20,955(1968); D.Cutts, et al., Phys.Rev. 184,1380 (1969); J.Bettels, et al., Nuovo Cimiento 56A,1106 (1968); D.Haidt, et al., Phys. Lett.29B,691(1969); D.Haidt, et al., Phys.Rev.D3,10(1971)

18. W.Morse, et al., Phys.Rev.D21,1750(1980)

19. S.MacDowell, Nuovo Cimiento 9,258(1958)

20. N.Cabibbo, A.Maksymowicz Phys.Lett.9,352(1964); Phys. Lett.11,360 (1964);Phys.Lett.14,72(1965)

21. L.Okun', I.Khriplovich Yad.Fiz.6,821(1967) [Sov.J.Nucl. Phys.6,598 (1968)]

22. A.Zhitnitskii, Yad.Fiz.31,1024(1980) [Sov.J.Nucl. Phys.31,529(1980)]

23. E.Ginsberg, Phys.Rev.D4,2893(1971)

24. J.Sakurai, Phys.Rev.109,980(1958)

25. S.Weinberg, Ref.10

26. A.Lahanas, Private communication

27. R.Baltrusaitis, F.Calaprice Phys.Rev.Lett.38,464(1977)

28. L.Leipuner, et al., IEEE Trans.Nucl.Sci. NS-28,1,333 (1981); ibid,1,369(1981); ibid,1,410(1981)

29. M.Campbell, doctoral thesis, Yale University, 1982(unpublished)

30. S.Hayakawa, Phys.Rev.108,1533(1957)

31. A.Buhler et al., Nuovo Cimicnto 39,824(1965)

32. The Dubna fitting program FUMILI was adapted by Dr. G. Takhtamyshev for use on the PDP-11 computer.

LIST OF FIGURES

the 48 blocks and the dimensions of the beam hole in the center.

Figure 9. Schematic representation of the electronic circuitry. The eight boxes along the bottom represent modules on the FASTBUS system, and the lines connecting them below indicate the sequence of interchanges on the FASTBUS during a typical event.

Figure 10. A definition of ϕ, the initial azimuthal angle of the muon polarization component about the beam axis, as measured from the normal to a positron counter (U or D).

Figure 11. Asymmetry as a function of time (all events).

a) CP conserving

b) CP violating

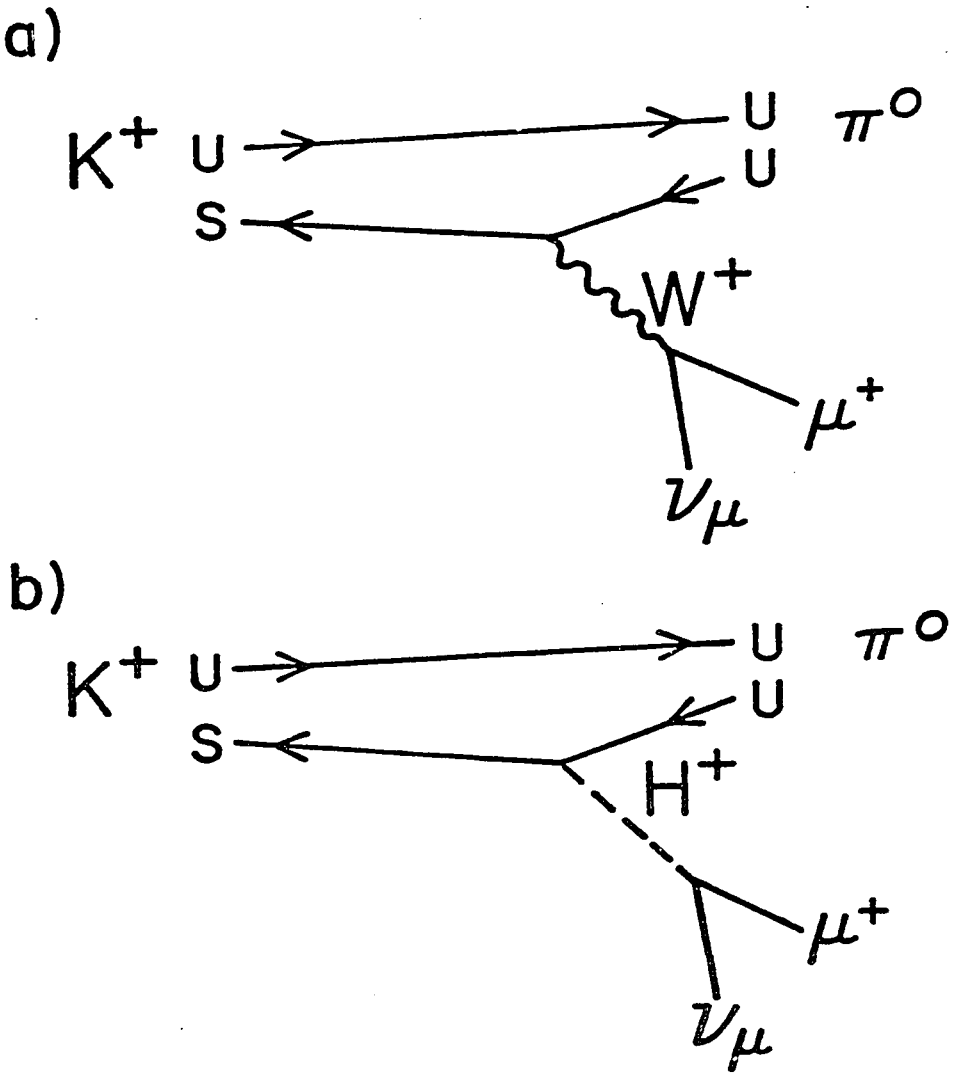

Figure 1. a)The $K^+_{\mu 3}$ decay mediated by a W boson

b)The $K^+_{\mu 3}$ decay mediated by a Higgs boson

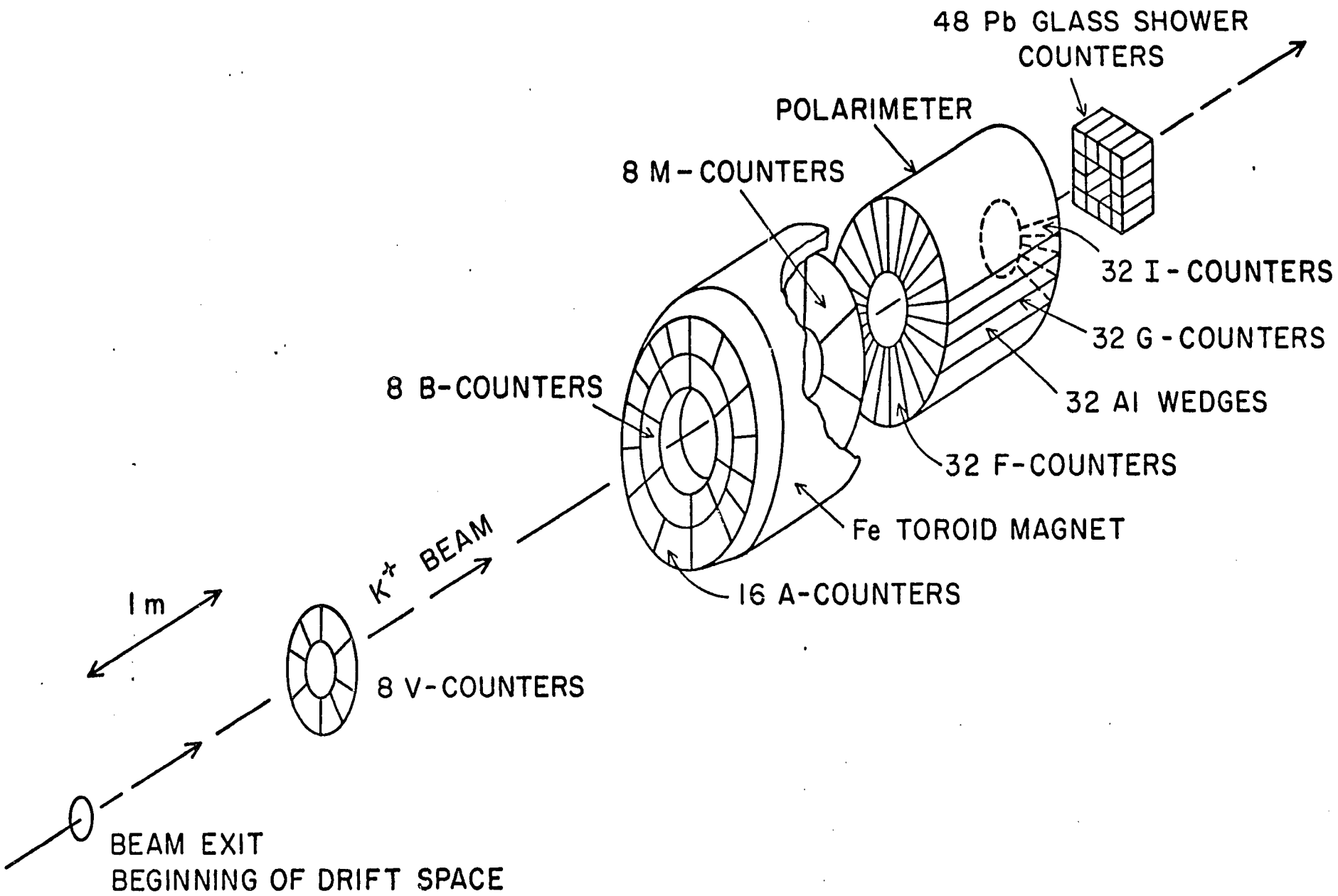

Figure 2. A schematic representation of the experimental apparatus.

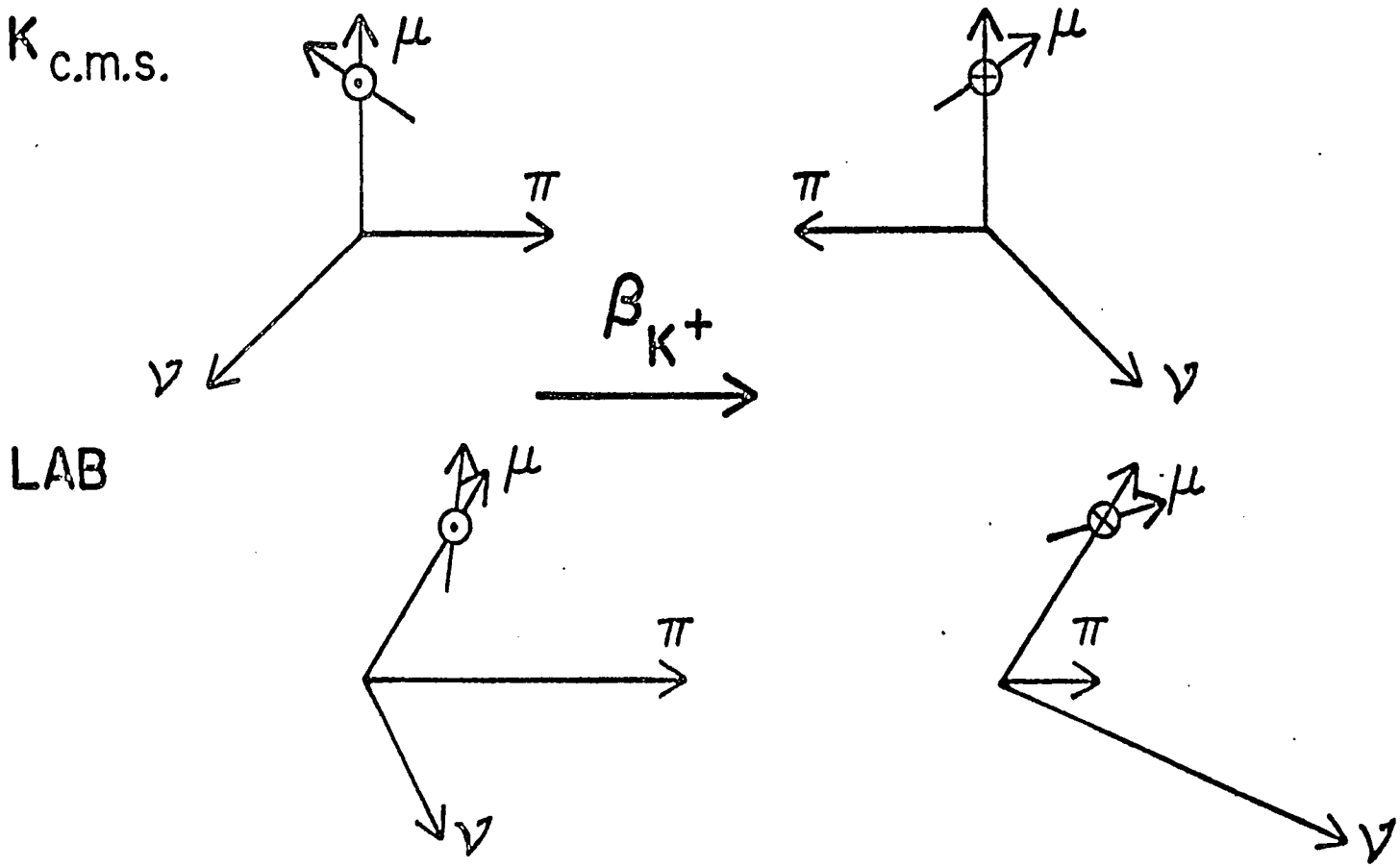

Figure 3. Two orientations of the decay products and the muon polarization, in the kaon rest frame and in the laboratory system.

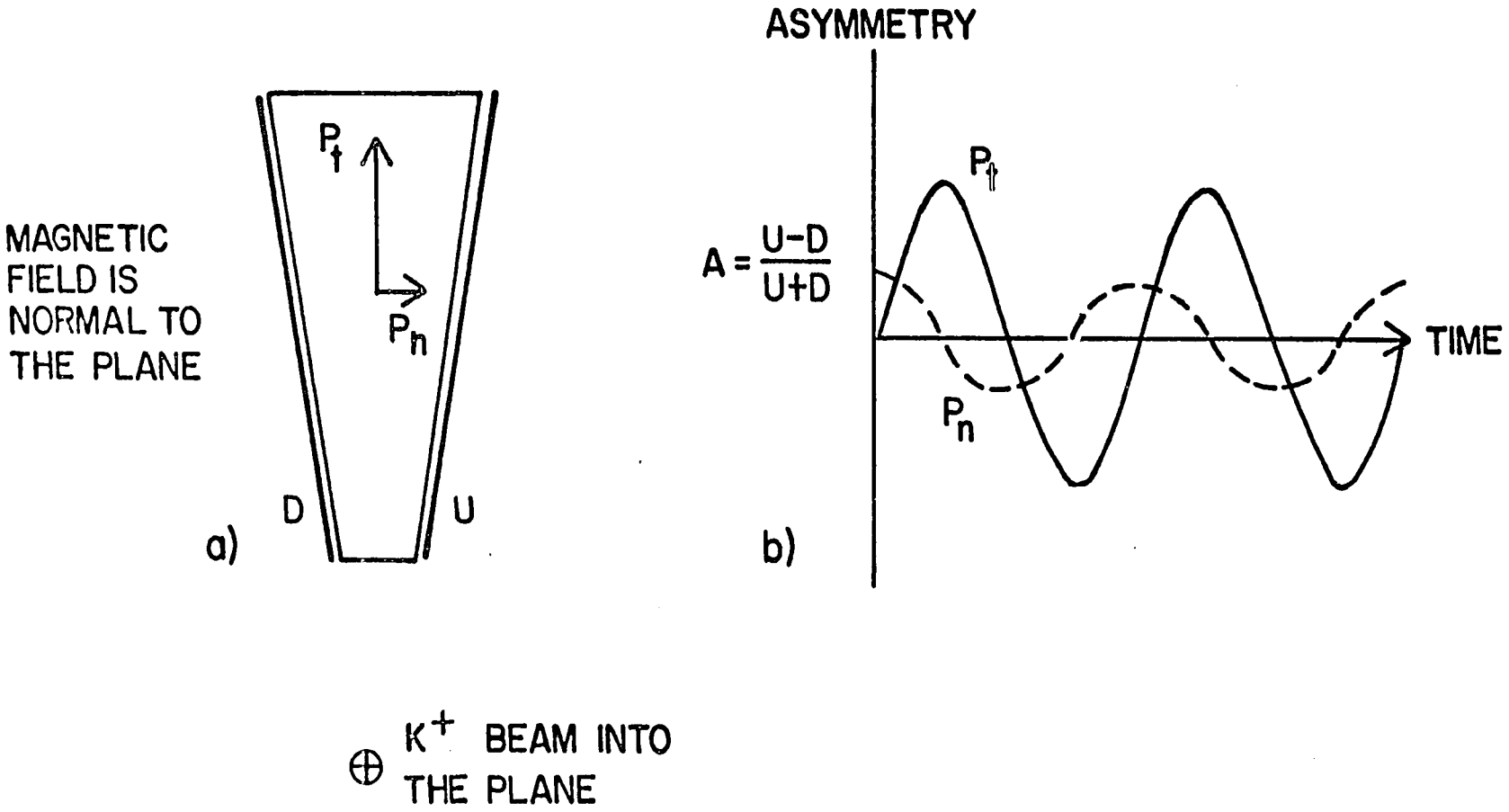

Figure 4. a) Schematic representation of the components of muon polarization in the polarimeter, as seen along the beam line.
b) Schematic representation of the contributions of the transverse polarizations to the asymmetry for an ensemble of precessing muons.

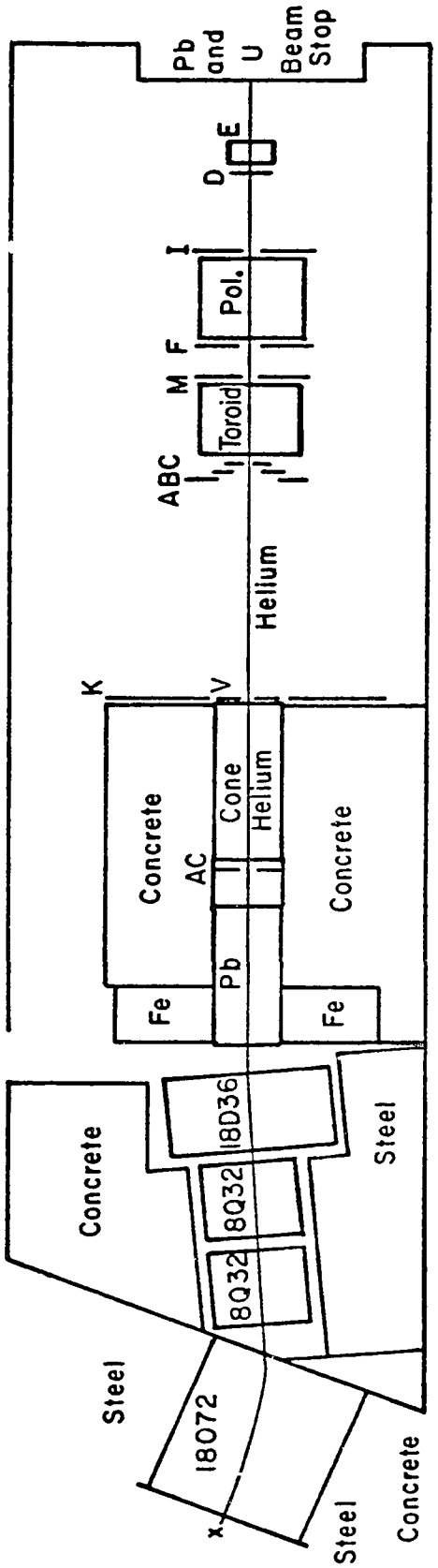

Figure 5. Layout of the magnets and experimental apparatus.

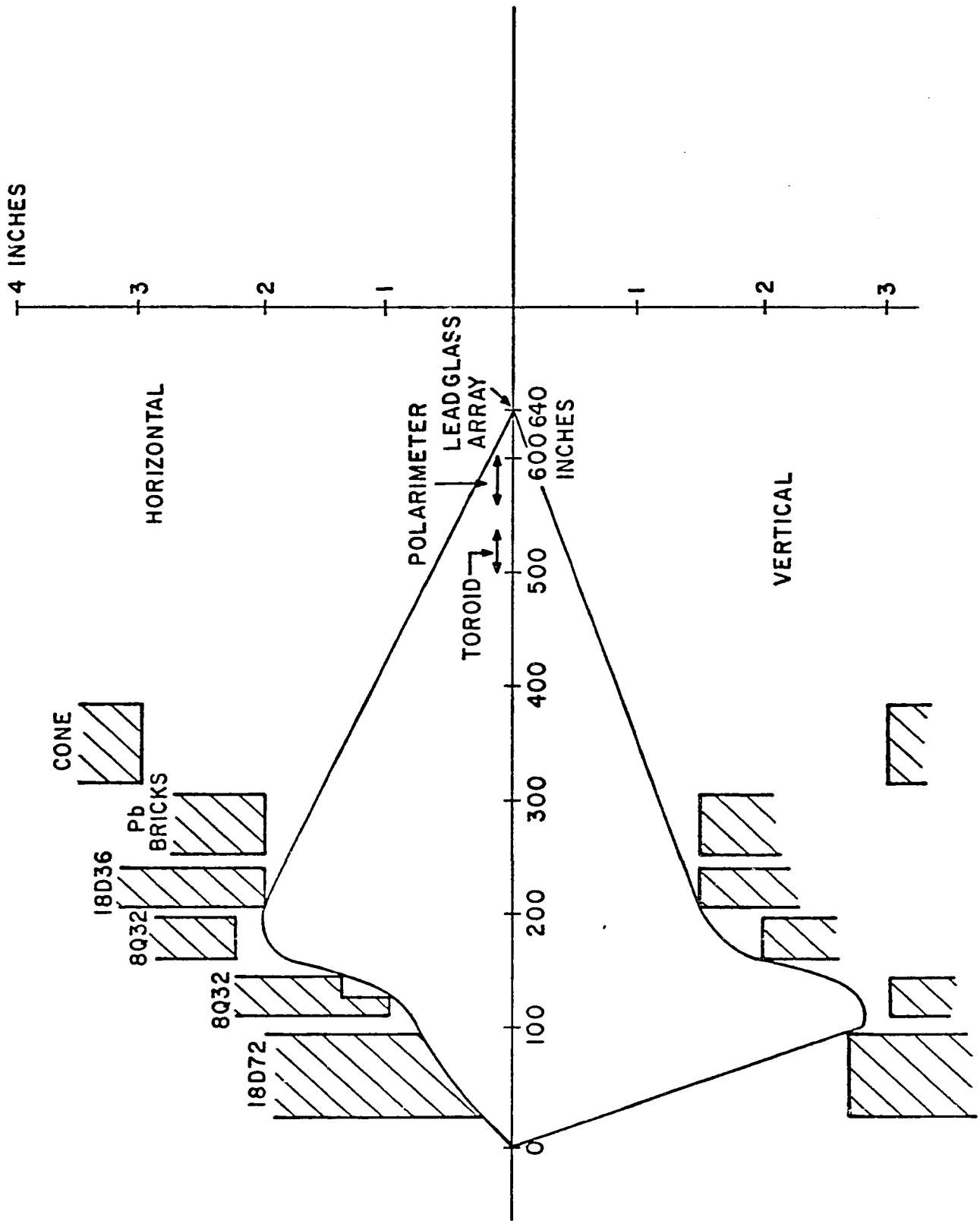

Figure 6. The collimators and beam optics for the 4 GeV beam line. The horizontal and vertical sections are shown separately. Note the foreshortened scale. The position of the toroid, polarimeter, and calorimeter are indicated by arrows at the appropriate point on the main axis.

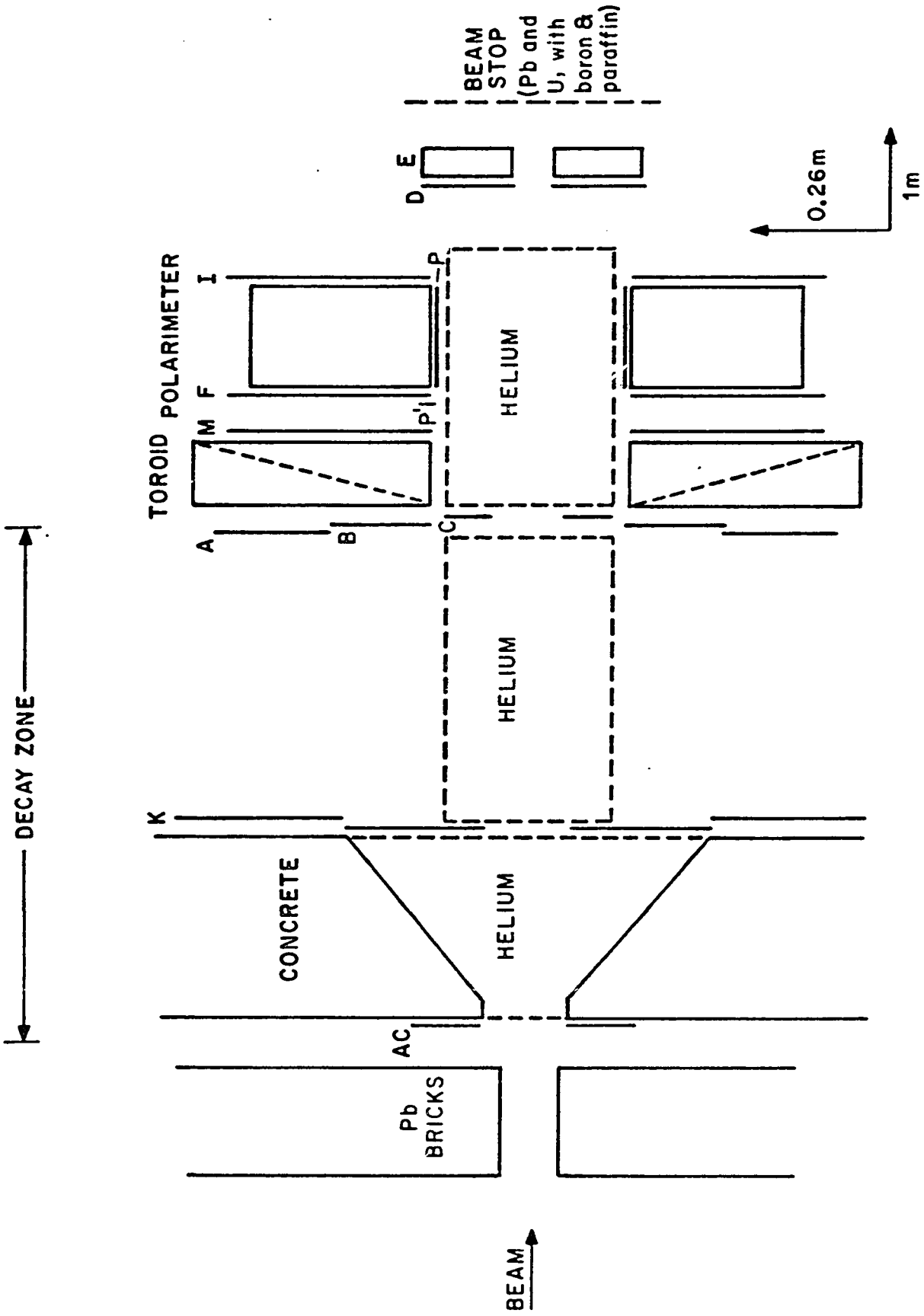

Figure 7. A layout of the detector cave (note the foreshortened scale) indicating the sizes and locations of the scintillation counter arrays and the lead glass array(E).

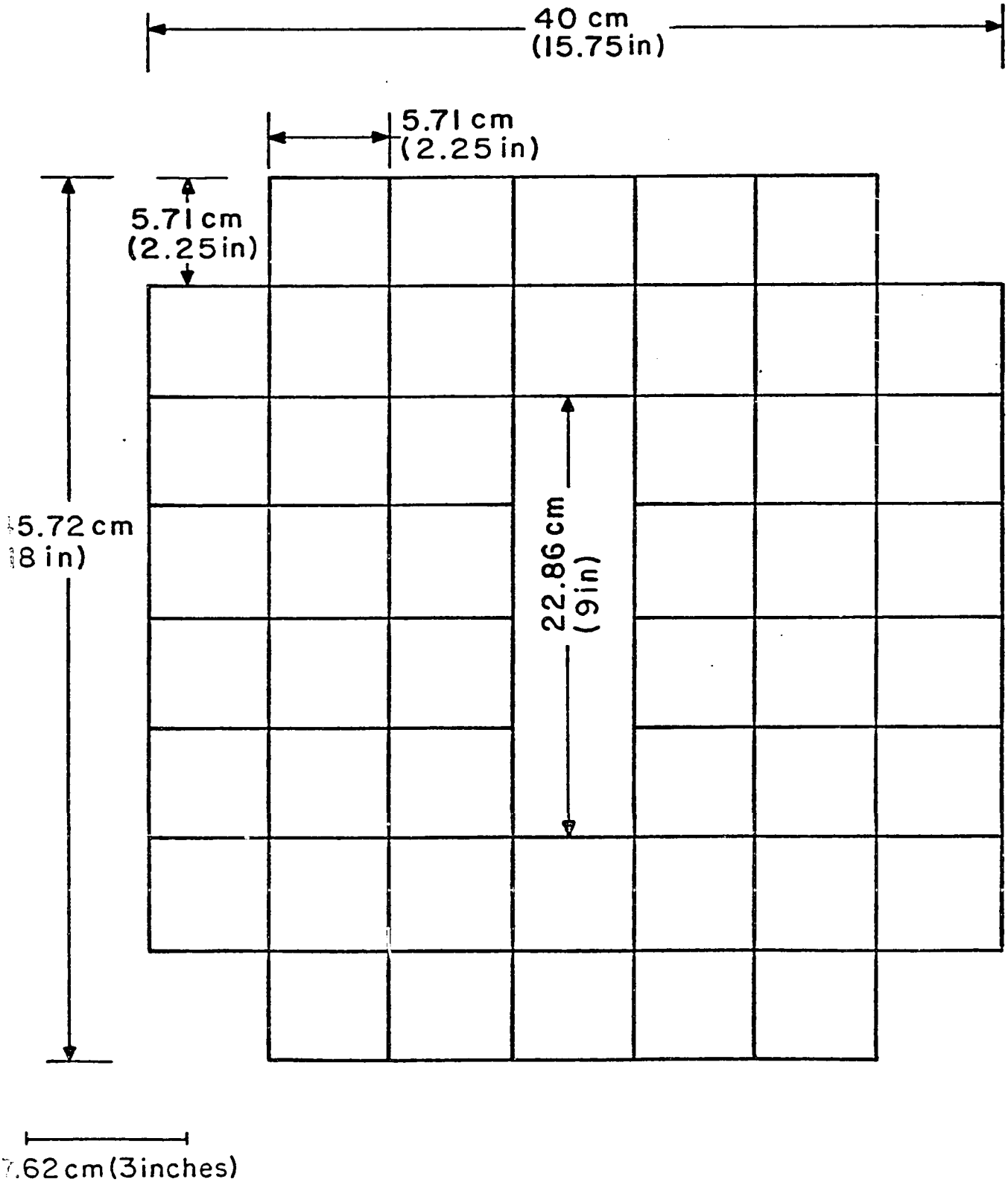

Figure 3. The face of the lead glass array, showing the layout of the 48 blocks and the dimensions of the beam hole in the center.

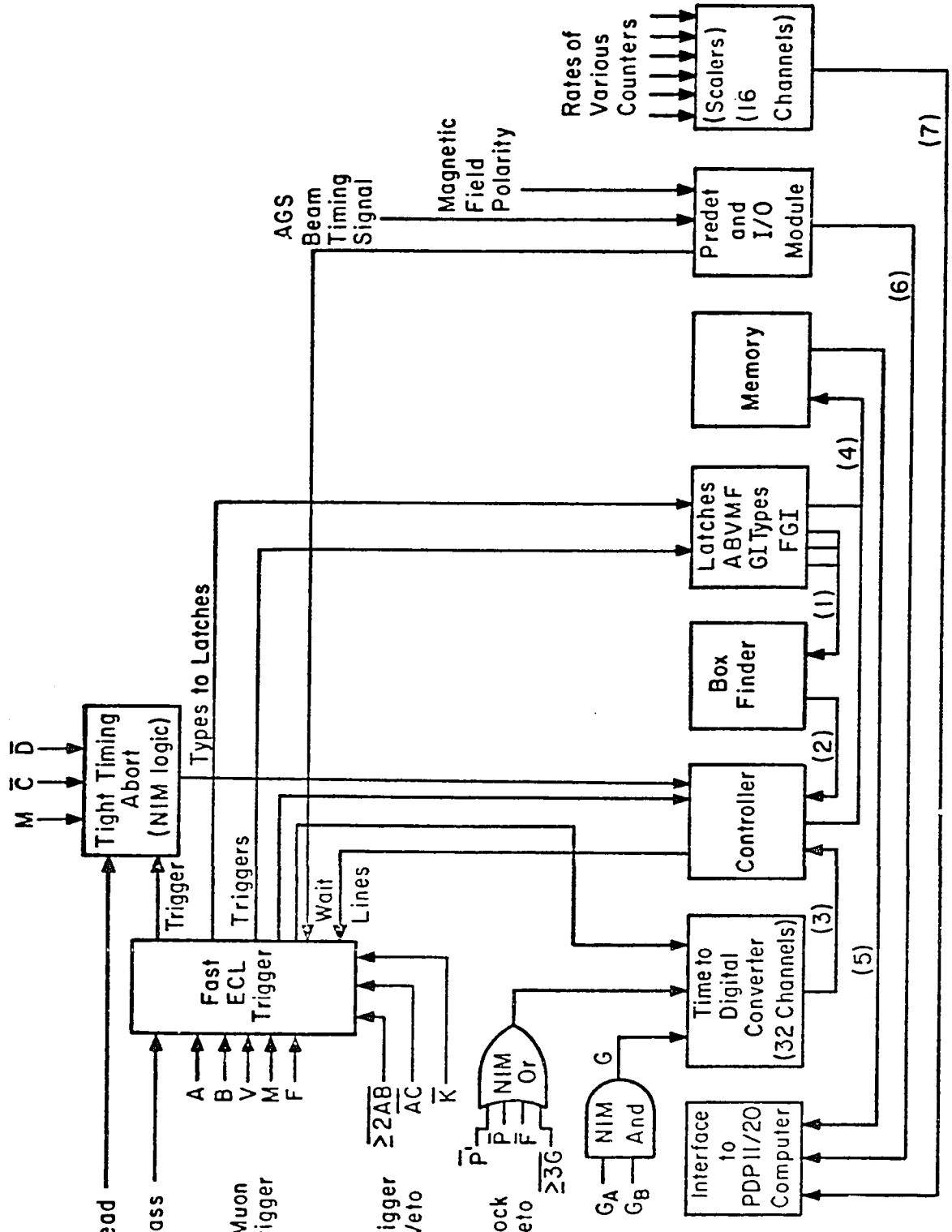

Figure 9. Schematic representation of the electronic circuitry. The eight boxes along the bottom represent modules on the FASTBUS system, and the lines connecting them below indicate the sequence of interchanges on the FASTBUS during a typical event.

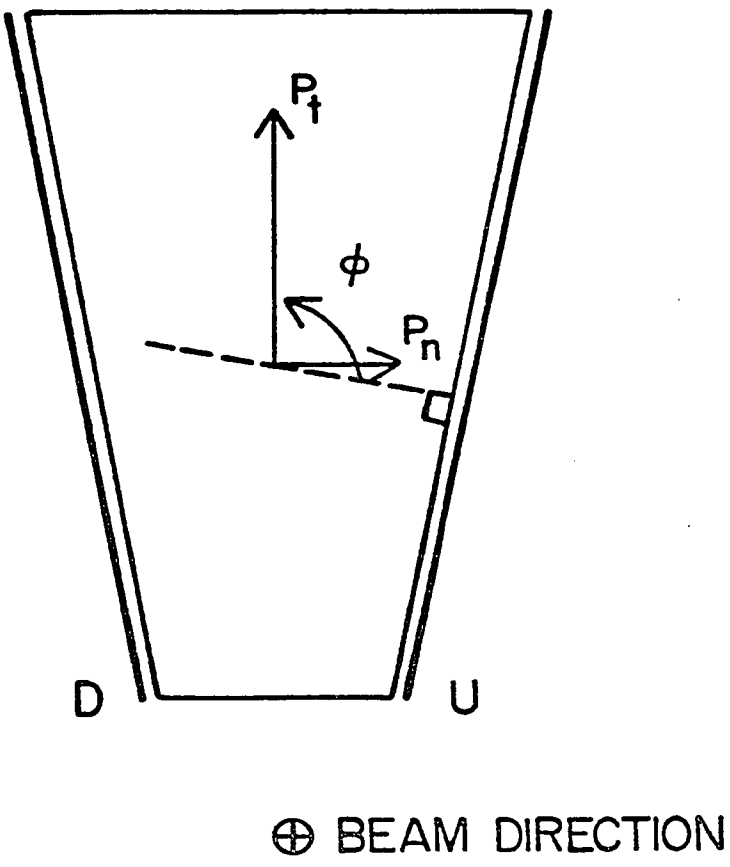

Figure 10. A definition of ϕ, the initial azimuthal angle of the muon polarization component about the beam axis, as measured from the normal to a positron counter (U or D).

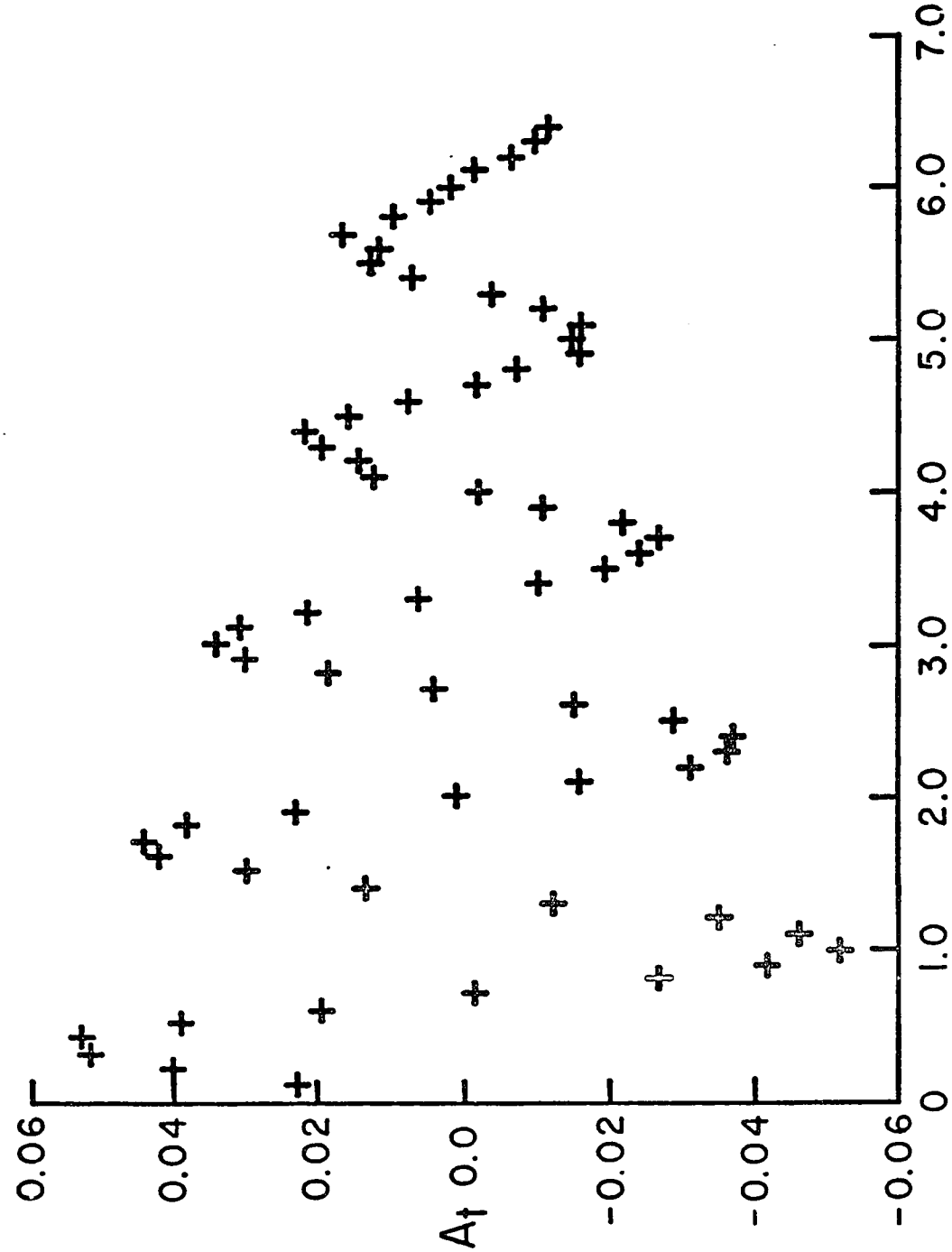

Figure 11. a) Asymmetry as a function of time (all events): CP conserving.

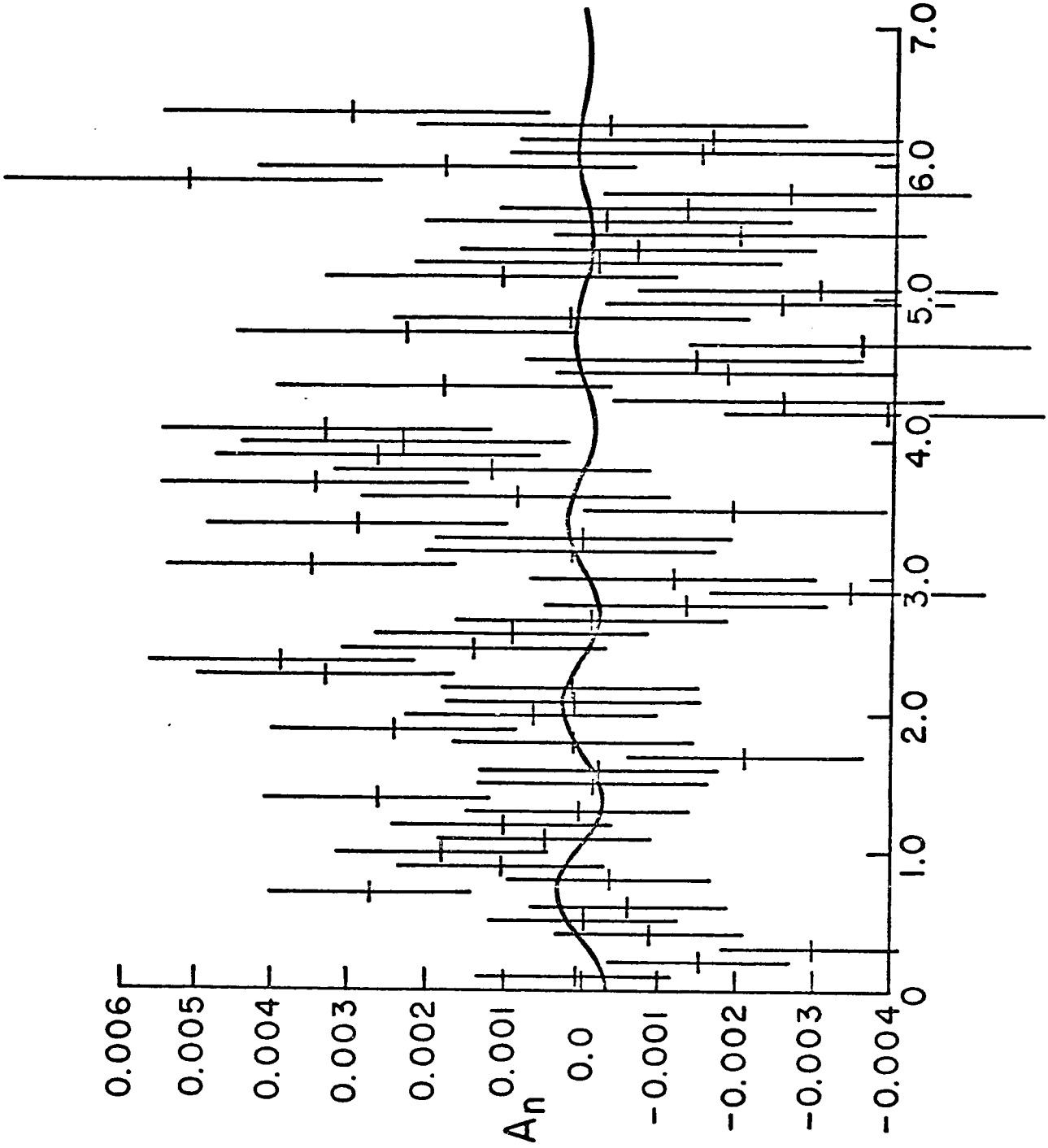

Figure 11. b) Asymmetry as a function of time (all events): CP violating.

LIST OF TABLES

Table 1

Monte Carlo Results

Type	AV	BV	A	B	All
Intensity(%)	35.1	12.4	8.4	44.1	100.0
$\langle P_t(\text{lab})\rangle$	0.728	0.586	0.787	0.783	0.740
$\langle P_n(\text{lab})\rangle$	0.00205	0.00155	0.00206	0.00191	0.00193
$\langle P_t(\text{CMS})\rangle$	0.673	0.812	0.574	0.612	0.655
$\langle P_n(\text{CMS})\rangle$	0.00259	0.00192	0.00313	0.00266	0.00258

with $\text{Re}\ \xi = 0.0$
$\text{Im}\ \xi = 0.01$

Table 2

Experimental Results

Type	Events (10^{-3})	$A_t(0)$	$A_n(0)$	Statistical Error
AV	5,201	0.0694	0.0022	0.0010
BV	2,951	0.0744	-0.0036	0.0022
A	3,829	0.0454	0.0009	0.0013
B	8,825	0.0922	-0.0018	0.0009
Total	20,806	0.0753	-0.00034	0.00058